Organometallic Ru, Os, Rh and Ir Half-Sandwich Conjugates of Ispinesib - Impact of the Organometallic Group on the Antimitotic Activity

Michał Łomzik[a], Andrzej Błauż[b], Marta Głodek[a], Anna Makal[c], Daniel Tchoń[c,f], Daniel Moscoh Ayine-Tora[d], Christian Hartinger[e], Błażej Rychlik[b], Damian Plażuk[a*]

[a] *Department of Organic Chemistry, Faculty of Chemistry, University of Lodz, ul. Tamka 12, 91-403 Łódź, Poland*

[b] *Cytometry Lab, Department of Oncobiology and Epigenetics, Faculty of Biology and Environmental Protection, University of Lodz, University of Lodz, ul. Pomorska 141/143, W24, 90-236 Łódź, Poland*

[c] *Laboratory for Structural and Biochemical Research (LBSBio), Biological and Chemical Research Centre, Department of Chemistry, University of Warsaw, ul. Zwirki i Wigury 101, 02-089 Warszawa, Poland*

[d] *Department of Chemistry, University of Ghana, LG 56, Legon-Accra, Ghana*

[e] *School of Chemical Sciences, The University of Auckland, Private Bag 92019, Auckland 1142, New Zealand*

[f] *Molecular Biophysics and Integrated Bioimaging Division, Lawrence Berkeley National Laboratory, Berkeley, CA 94720, USA*

Table of Contents

Copies of DOSY spectra

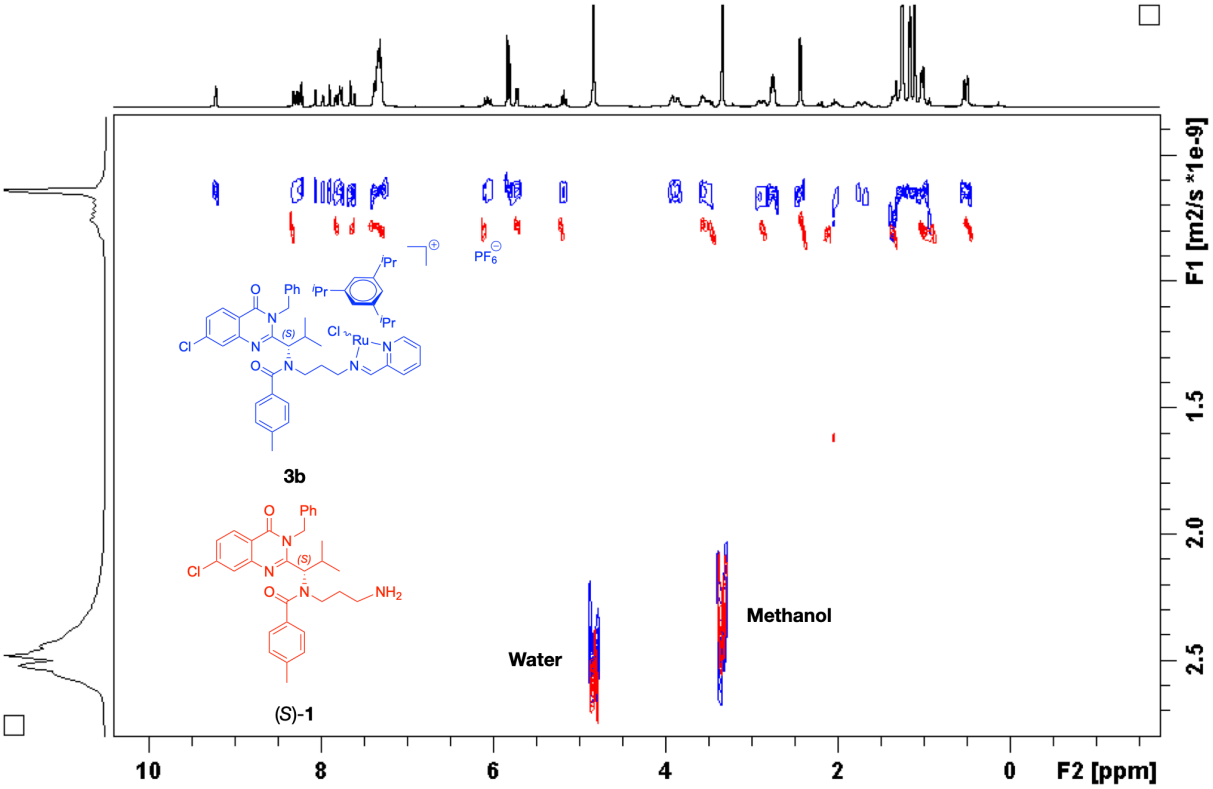

Supporting Figure S1. Overlaid ^{1}H DOSY spectra of **3b** and (*S*)-**1** in methanol-d$_4$

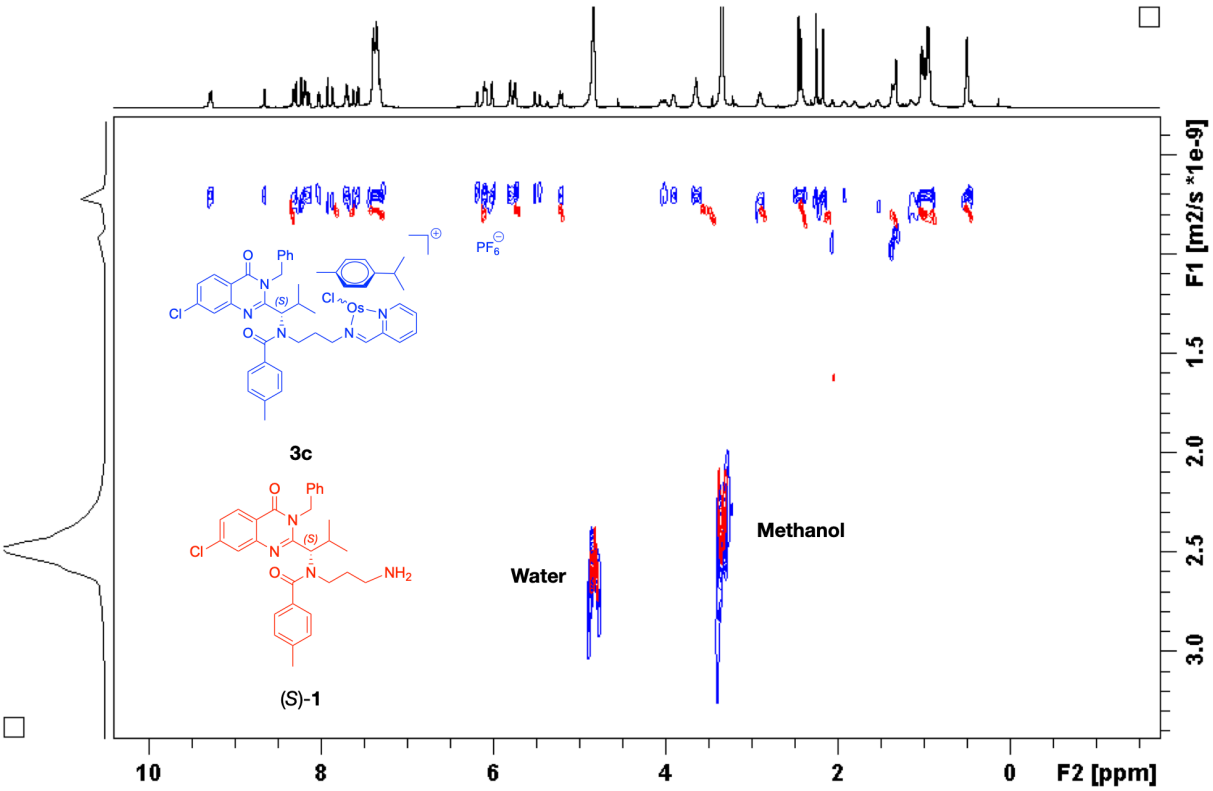

Supporting Figure S2. Overlaid ^{1}H DOSY spectra of **3c** and (*S*)-**1** in methanol-d$_4$

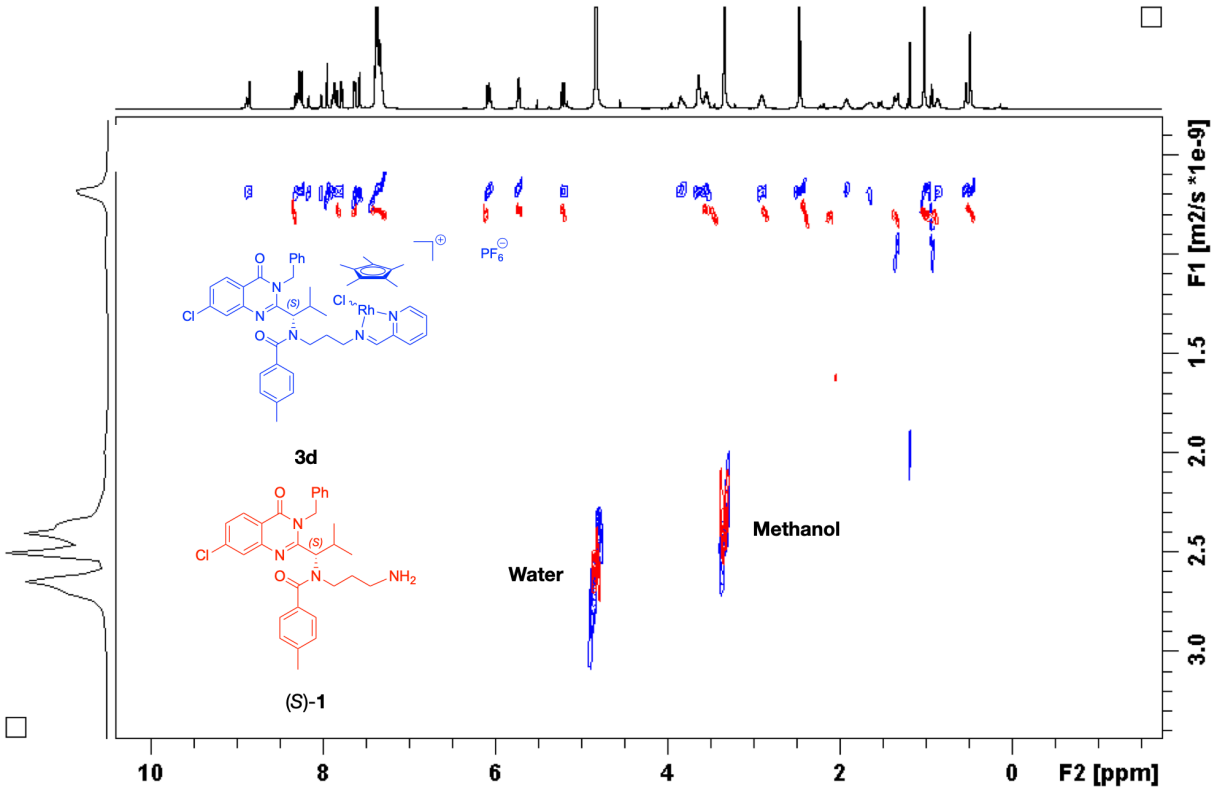

Supporting Figure S3. Overlaid ^{1}H DOSY spectra of **3d** and (*S*)-**1** in methanol-d$_4$

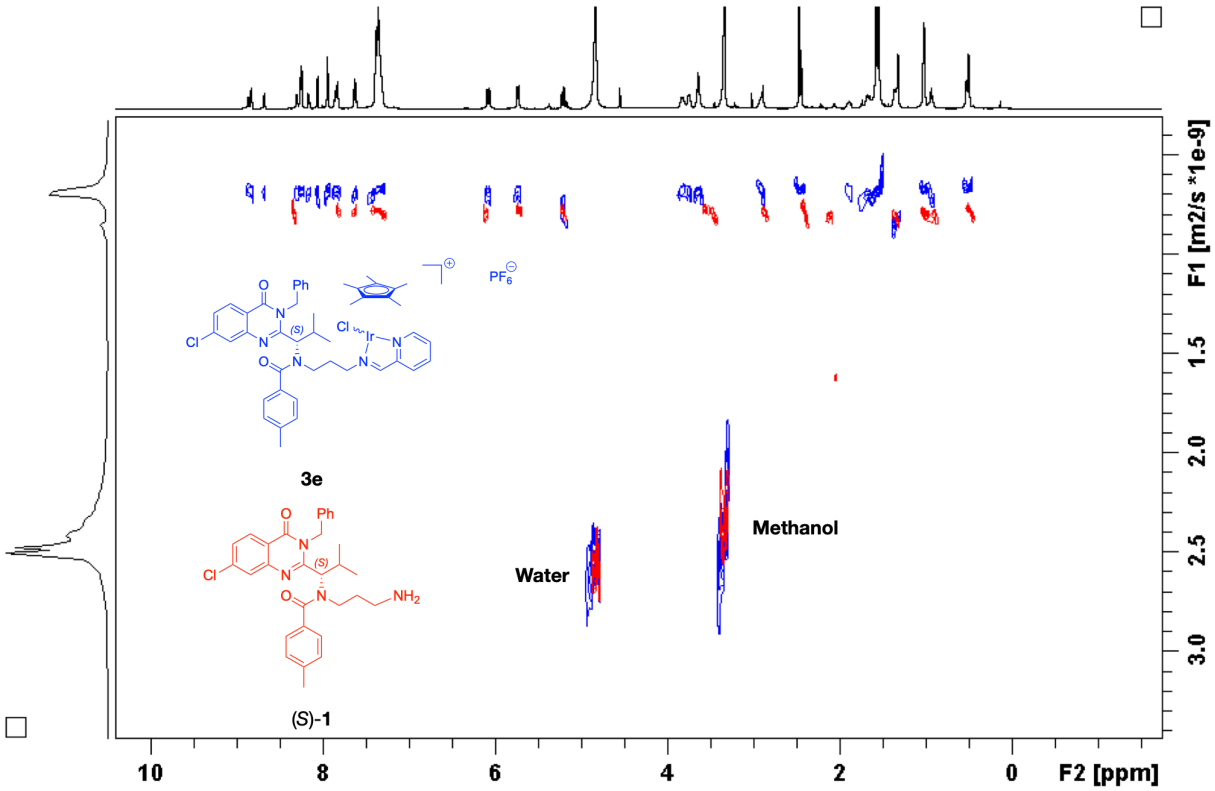

Supporting Figure S4. Overlaid ^{1}H DOSY spectra of **3e** and (*S*)-**1** in methanol-d$_4$

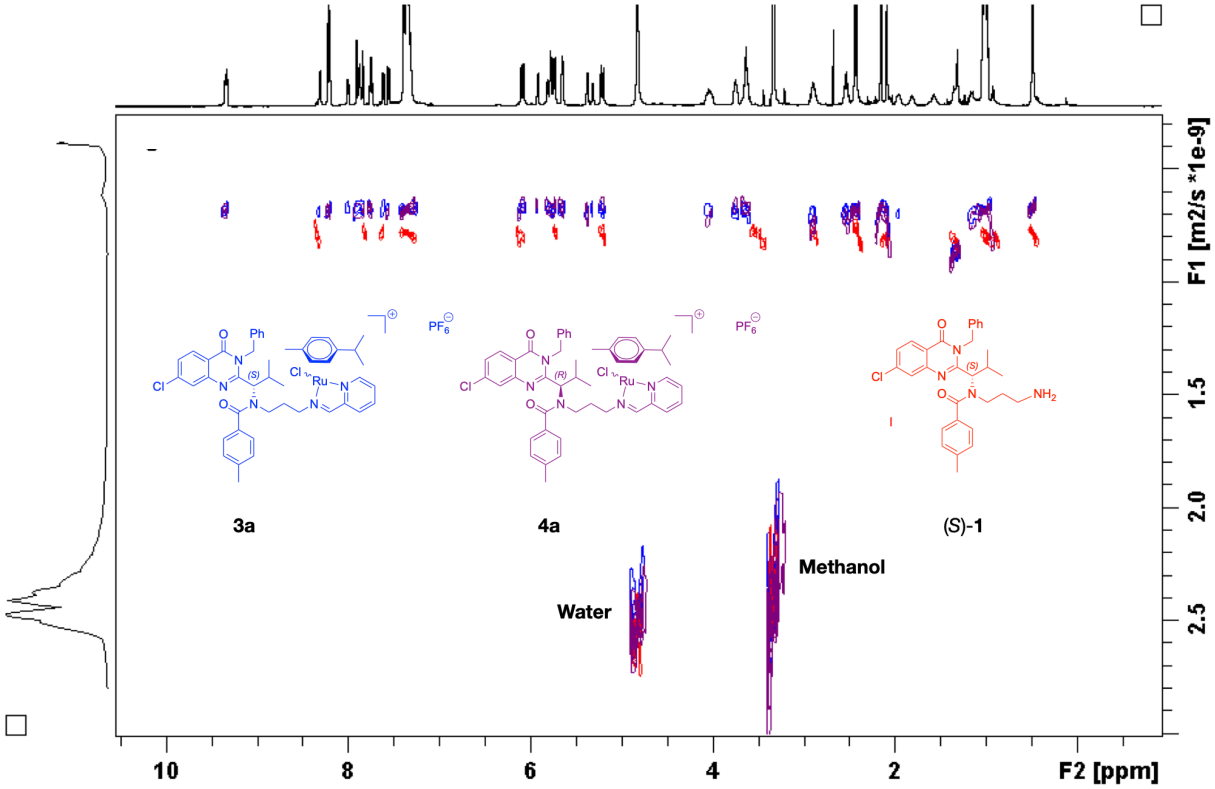

Supporting Figure S5. Overlaid ^{1}H DOSY spectra of **3a**, **4a** and (*S*)-**1** in methanol-d$_4$

LC-MS Analysis

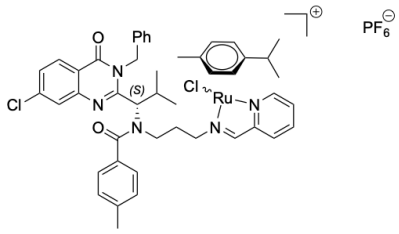

3a

$PF_6^{\ominus}$

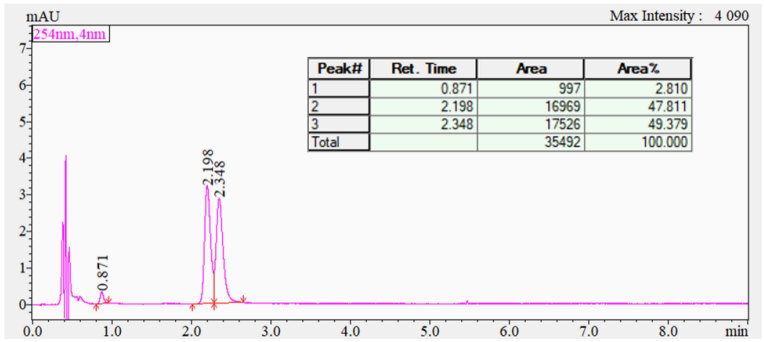

m/z [**3a** - $PF_6^{\ominus}$]$^+$

Chemical Formula: $C_{46}H_{50}Cl_2N_5O_2Ru^+$

Exact Mass: 876.2

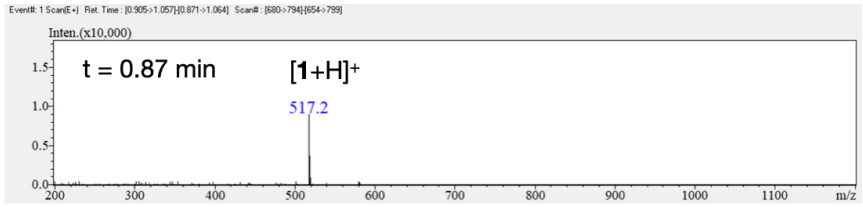

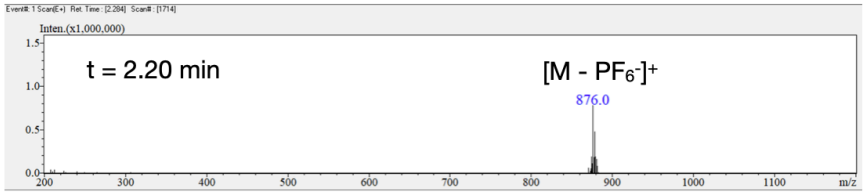

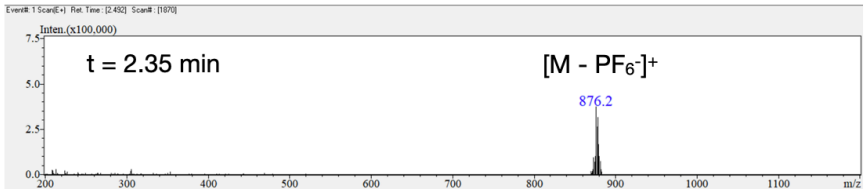

Supporting Figure S6. HPLC-MS analysis of **3a**

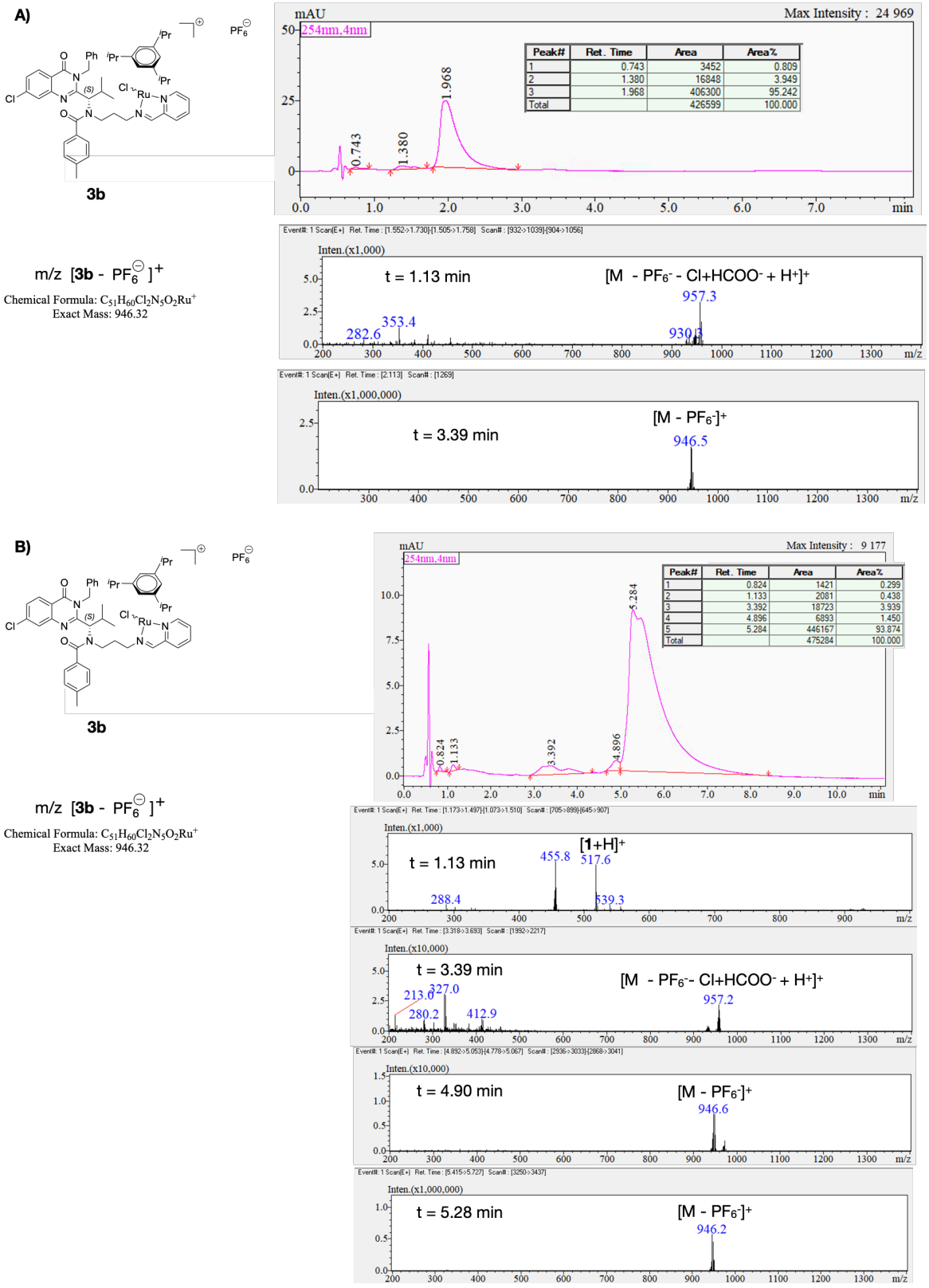

Supporting Figure S7. HPLC-MS analysis of **3b**. A) mobile phase 27.5% of MeOH and 27.5% MeCN in water + 0.01% of HCOOH as eluent with flow rate of 0.3 $mL \cdot min^{-1}$; B) mobile phase 65% of MeOH in water + 0.01% of HCOOH as eluent with flow rate of 0.4 $mL \cdot min^{-1}$;

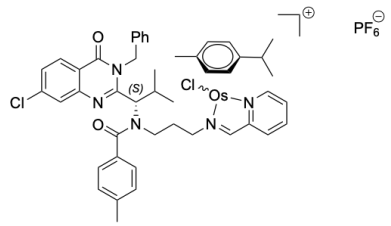

3c

m/z [**3c** - $PF_6^{\ominus}$]$^+$

Chemical Formula: $C_{46}H_{50}Cl_2N_5O_2Os^+$
Exact Mass: 966.3

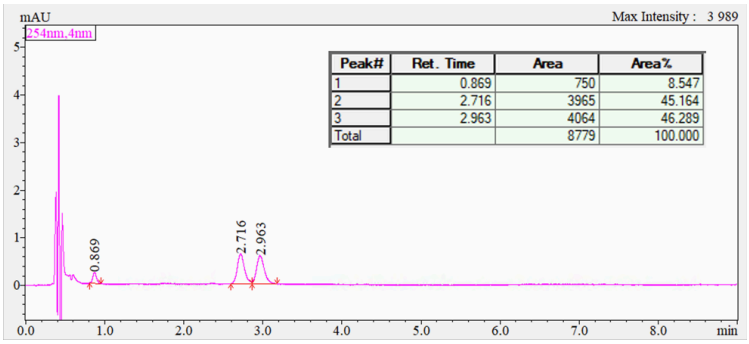

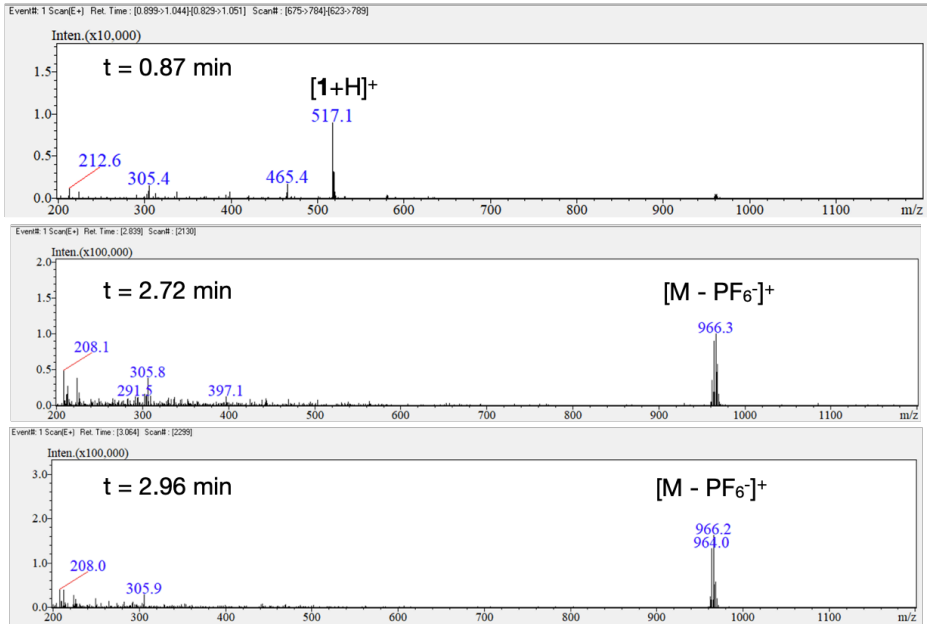

Supporting Figure S8. HPLC-MS analysis of **3c**

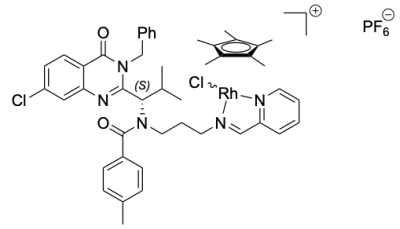

3d

m/z [**3d** - $PF_6^{\ominus}$]$^+$

Chemical Formula: $C_{46}H_{51}Cl_2N_5O_2Rh^+$
Exact Mass: 878.2

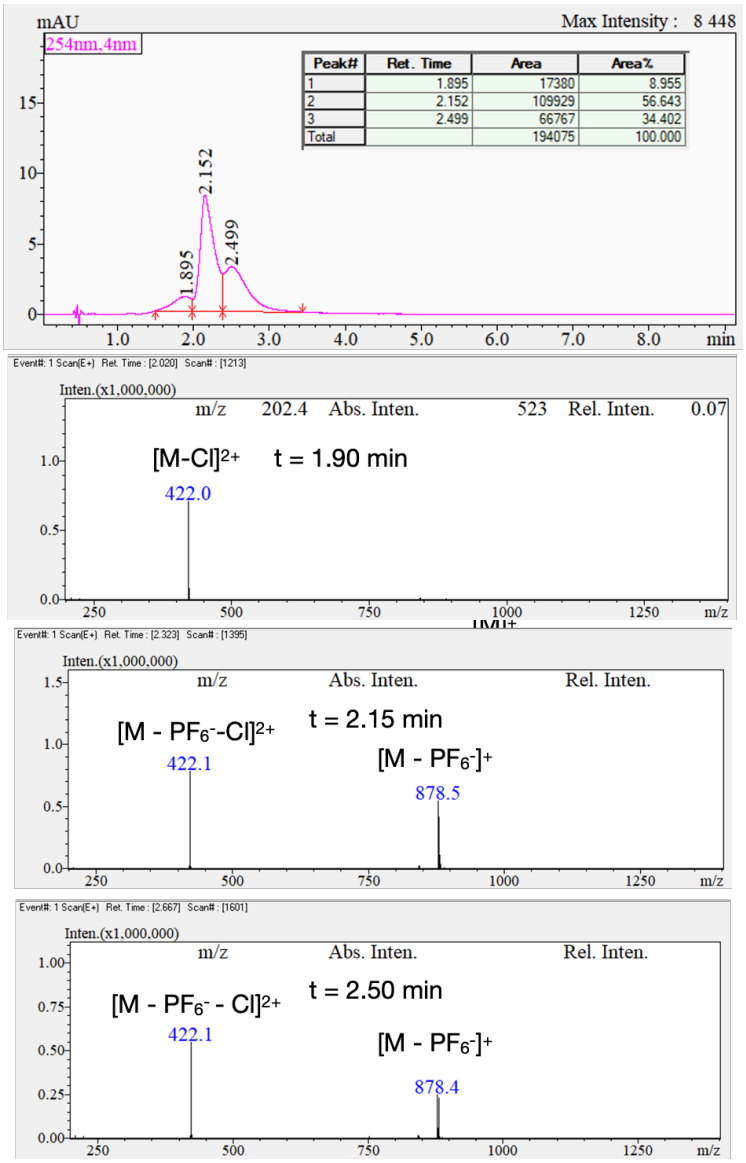

Supporting Figure S9. HPLC-MS analysis of **3d**

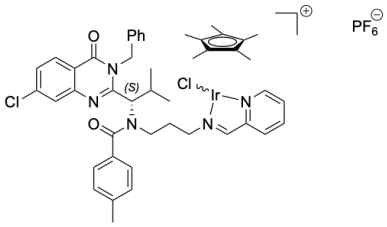

3e

m/z [**3e** - $PF_6^{\ominus}$]$^+$

Chemical Formula: $C_{46}H_{51}Cl_2IrN_5O_2^+$

Exact Mass: 968.30

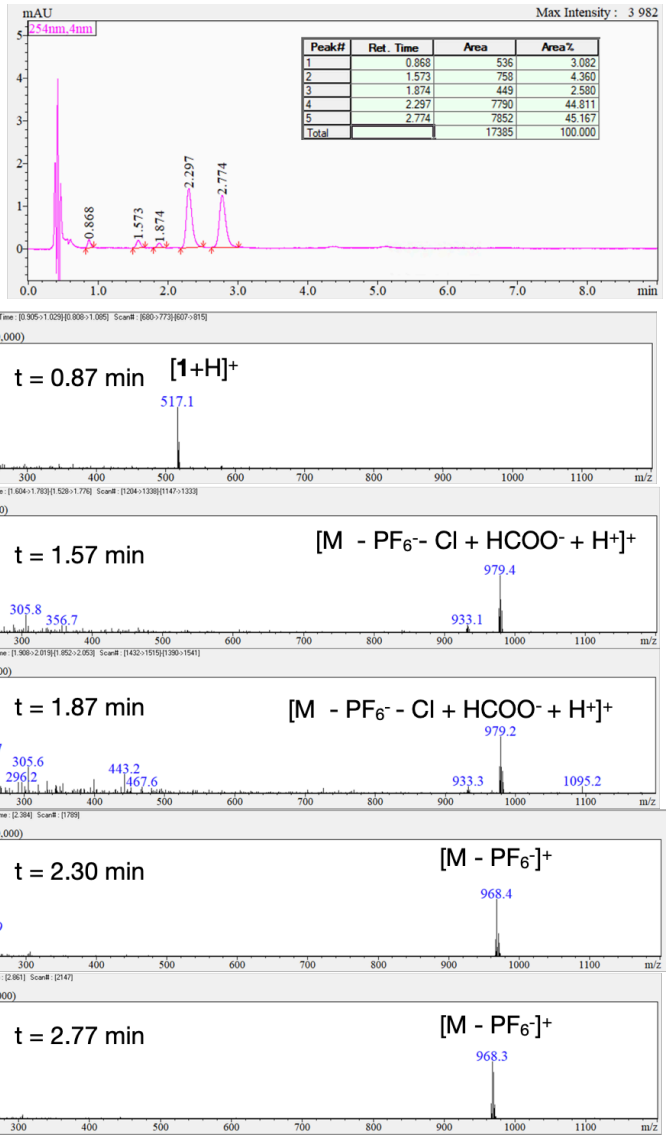

Supporting Figure S10. HPLC-MS analysis of **3e**

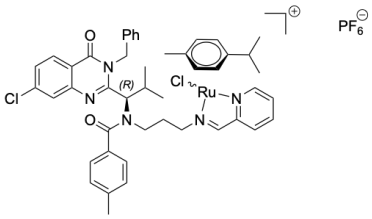

4a

m/z [**4a** - $PF_6^{\ominus}$]$^+$

Chemical Formula: $C_{46}H_{50}Cl_2N_5O_2Ru^+$

Exact Mass: 876.2

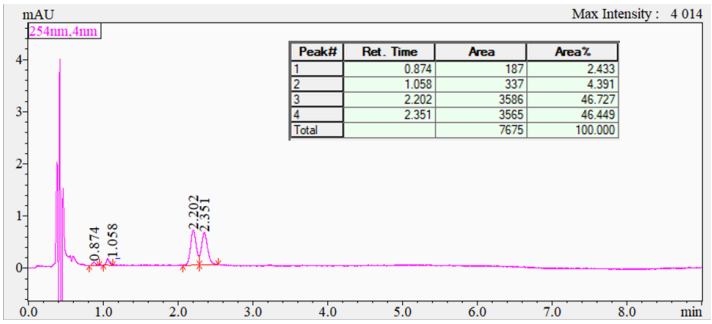

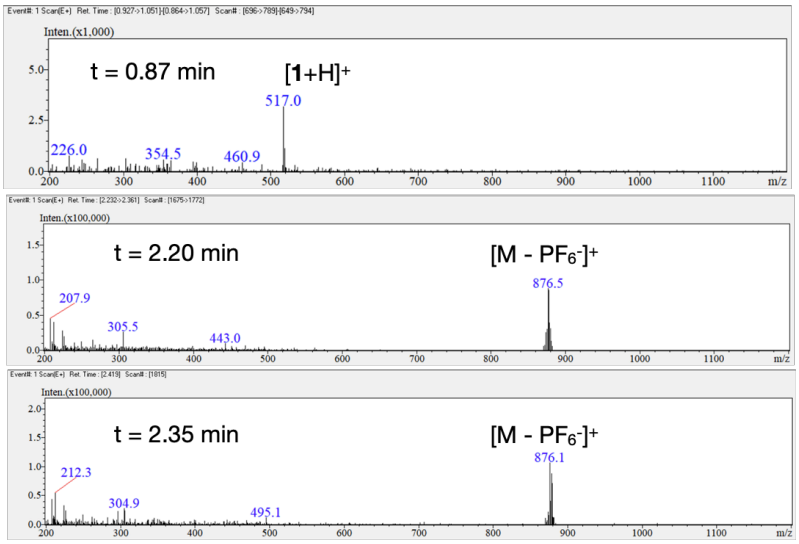

Supporting Figure S11. HPLC-MS analysis of **4a**

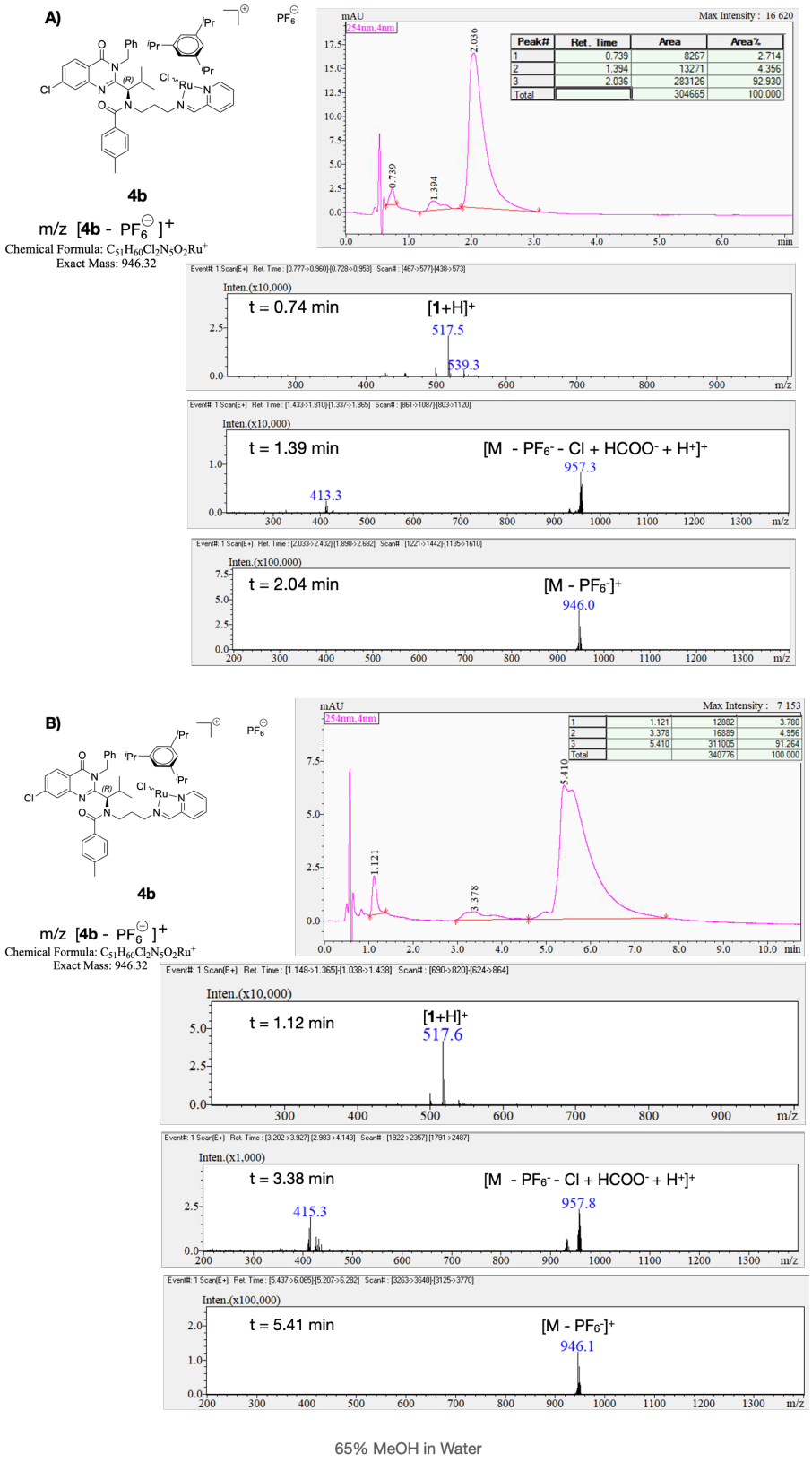

Supporting Figure S12 HPLC-MS analysis of **4b** A) mobile phase 27.5% of MeOH and 27.5% MeCN in water + 0.01% of HCOOH as eluent with flow rate of 0.3 mL·min^{-1}; B) mobile phase 65% of MeOH in water + 0.01% of HCOOH as eluent with flow rate of 0.4 mL·min^{-1};

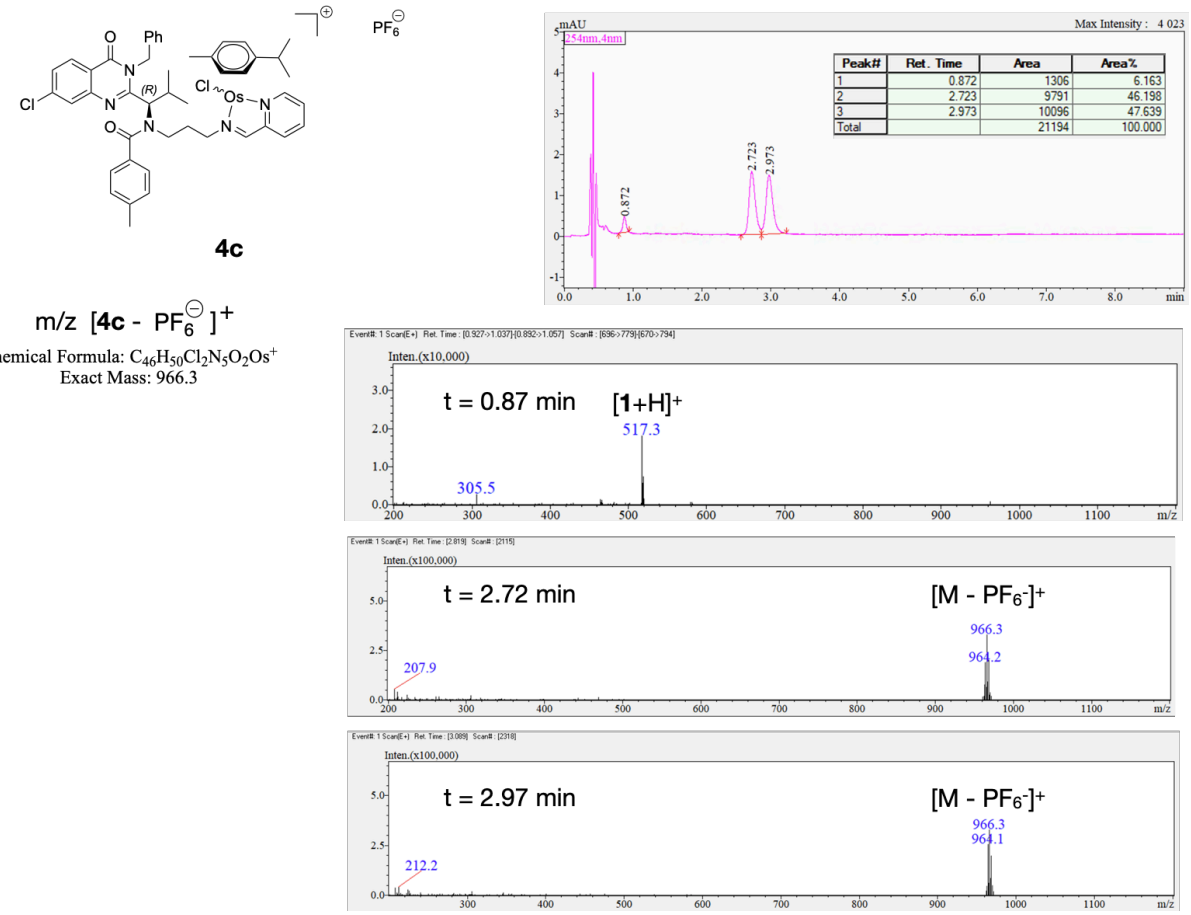

Supporting Figure S13. HPLC-MS analysis of **4c**

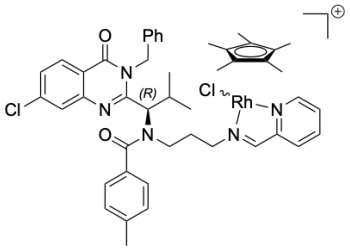

4d

m/z [**4d** - $PF_6^{\ominus}$]$^+$

Chemical Formula: $C_{46}H_{51}Cl_2N_5O_2Rh^+$
Exact Mass: 878.25

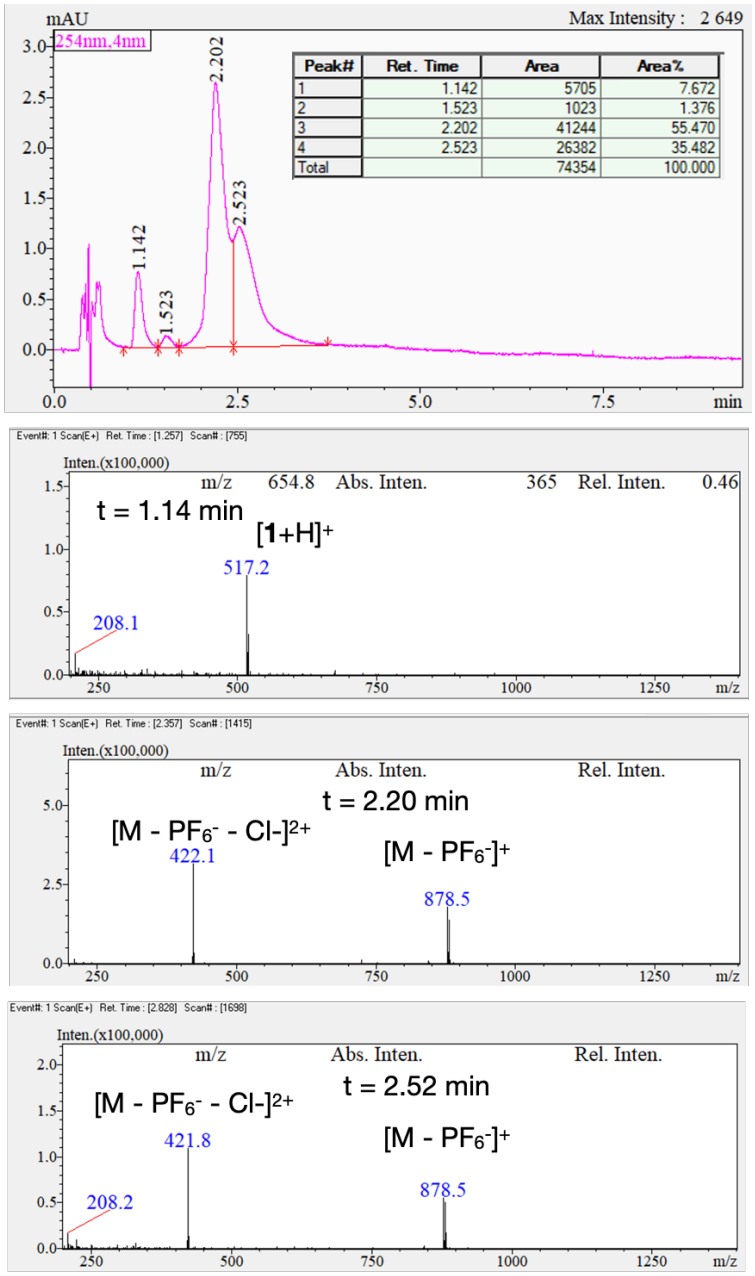

Supporting Figure S14. HPLC-MS analysis of **4d**

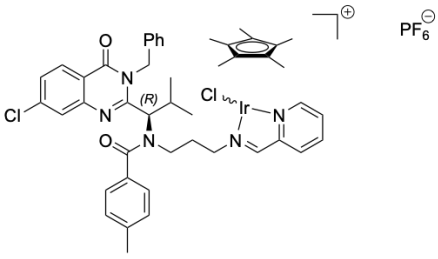

4e

m/z [**4e** - PF_6^-]$^+$

Chemical Formula: $C_{46}H_{51}Cl_2IrN_5O_2^+$
Exact Mass: 968.30

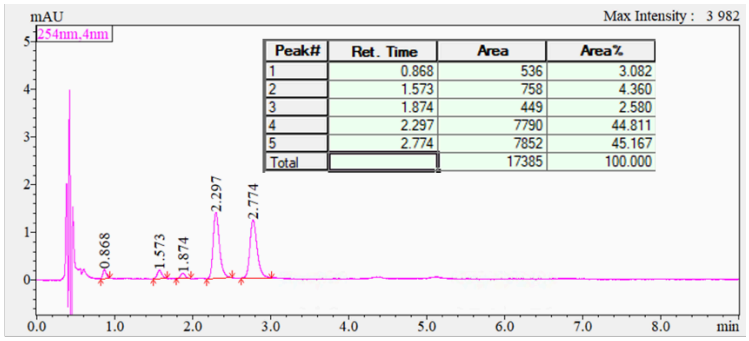

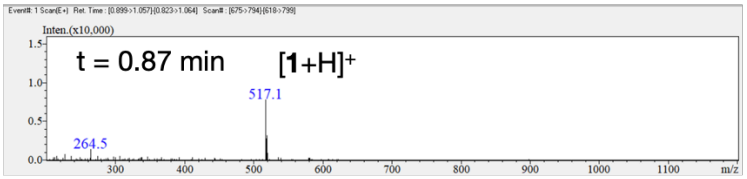

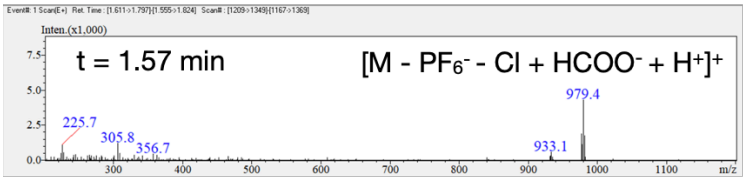

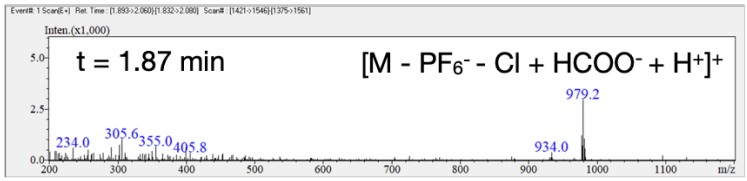

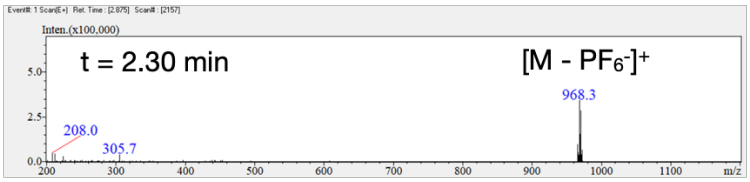

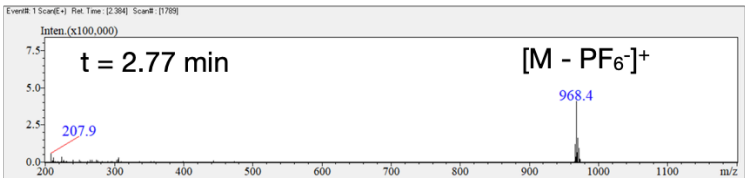

Supporting Figure S15. HPLC-MS analysis of **4e**

Table S1. Summary of the most important data and structure for **3e**$^{S,R_{Ir}}$·CH_2Cl_2**.**

Compound	**3e**$^{S,R_{Ir}}$
Empirical formula	$C_{46}H_{51}Cl_2IrN_5O_2F_6P·CH_2Cl_2$
CCDC number	2207901
Formula weight	1198.91
Crystal system	monoclinic
Space group	$P2_1$
a/Å	8.6827(2)
b/Å	11.6490(3)
c/Å	25.0534(7)
α/°	90
β/°	89.971(2)
γ/°	90
Volume/Å^3	2534.02(11)
Z	2
ρ_{calc}mg/mm^3	1.571
F(000)	1200
μ/mm^{-1}	7.890
Max. transmission	0.901
Min. transmission	0.420
Absorption corr.	Gaussian
Crystal color	clear light yellow
Crystal habit	plate

Crystal size/mm	0.157 × 0.121 × 0.015
R_{int}	0.0432
R_{sigma}	0.0384
Index ranges: h	10 -10
k	14 -14
l	31 -31
Reflections collected	37198
2Θ range : max	77.034
min	1.763
Temperature/K	100.0(1)
X-ray wavelength/Å	1.54184
Independent refl. I > 2 σ(I)	10259
Independent refl.	10400
Largest diff.: peak /e $Å^{-3}$	5.482
hole /e $Å^{-3}$	-2.099
Goodness-of-fit on F^2	1.061
Parameters	604
Data	15726
Restraints	130
R1 all data	0.0489
R1 [I>=2σ (I)]	0.0481
wR2 all data	0.1125

wR2 [I>=2σ (I)]	0.1129
Flack parameter	-0.018(4)

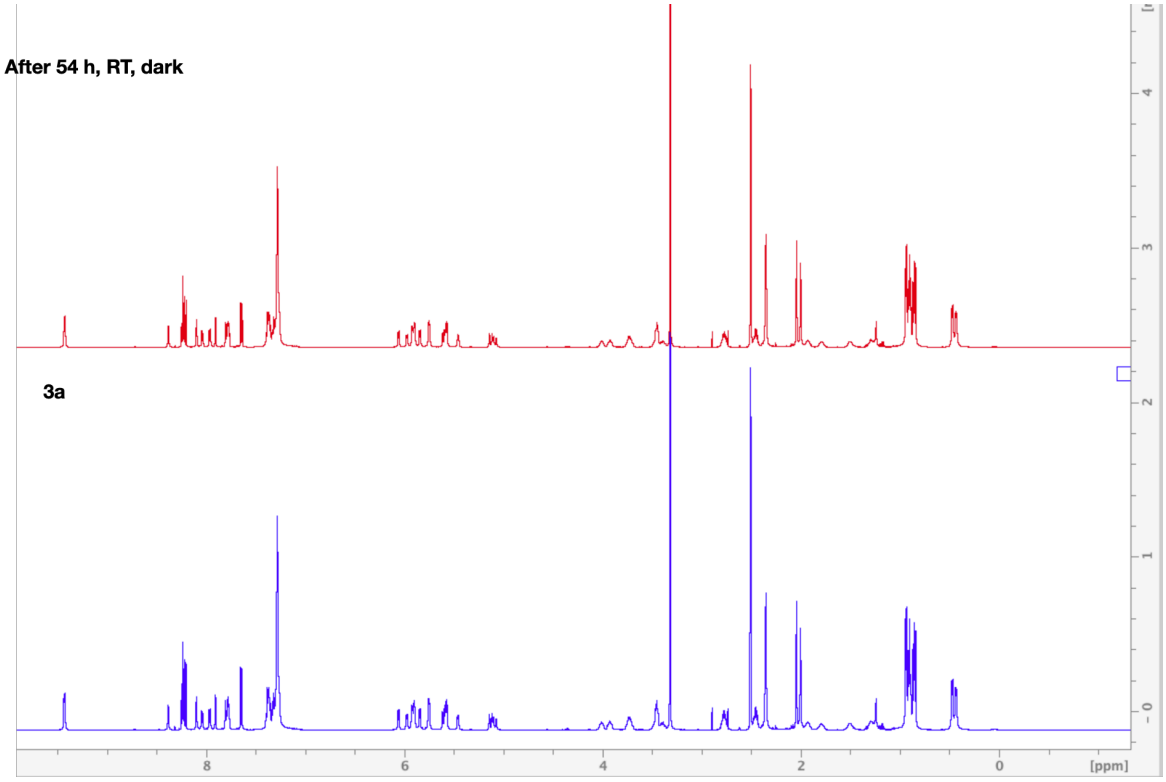

Supporting Figure S16. ^{1}H NMR spectra of **3a** in DMSO-d_6 - comparing fresh solution (blue) and solution after 54 h (red) at room temperature

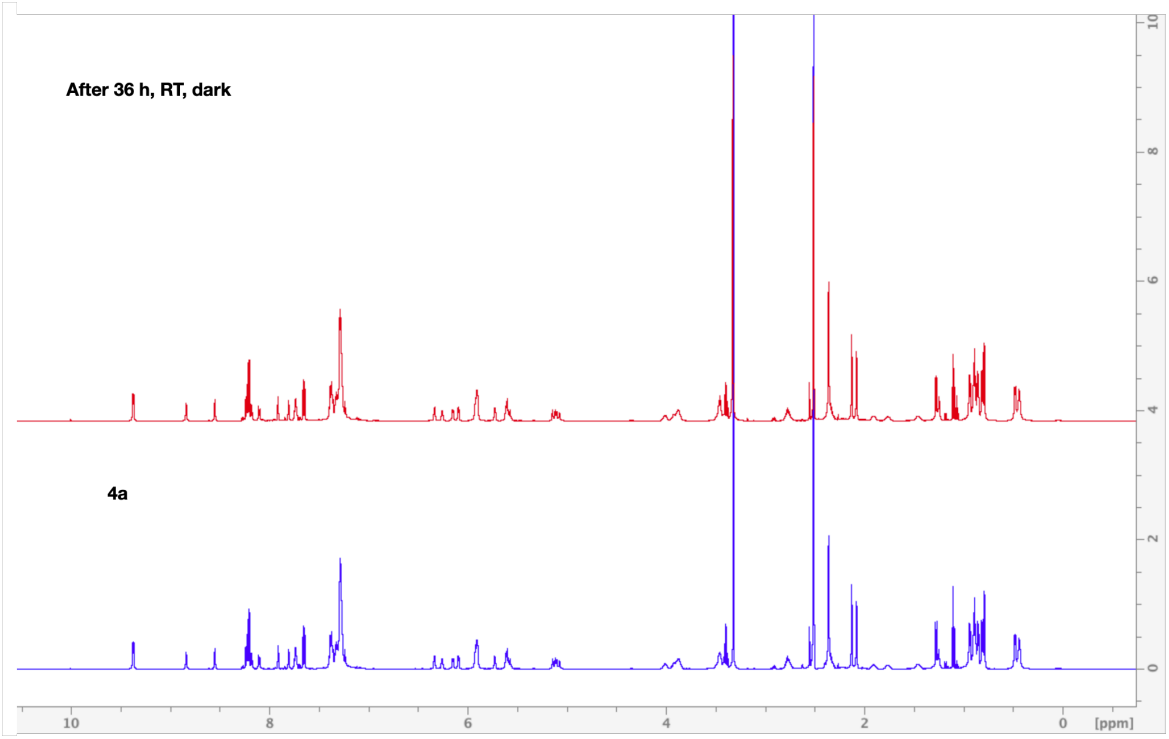

Supporting Figure S17. ^{1}H NMR spectra of **4a** in DMSO-d_6 - comparing fresh solution (blue) and solution after 36 h (red) at room temperature

ESI-MS analysis of the complexes in DMSO solution

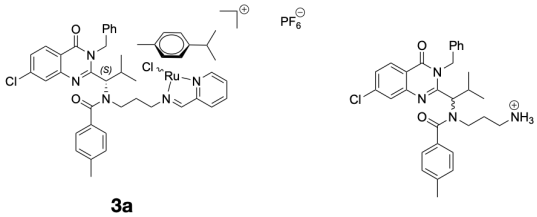

3a

m/z [**3a** - PF_6^-]$^+$

Chemical Formula: $C_{46}H_{50}Cl_2N_5O_2Ru^+$
Exact Mass: 876.2

m/z [**1**+H]$^+$

Chemical Formula: $C_{30}H_{34}ClN_4O_2^+$
Exact Mass: 517.2

ESI-MS Analysis of 3a in DMSO - direct injection

t = 0 min m/z extracted from TIC chromatogram

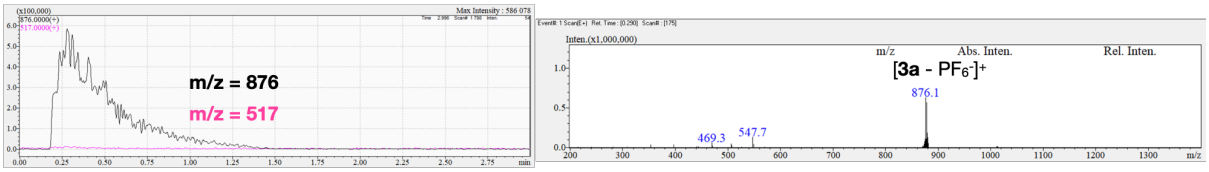

t = 24 h

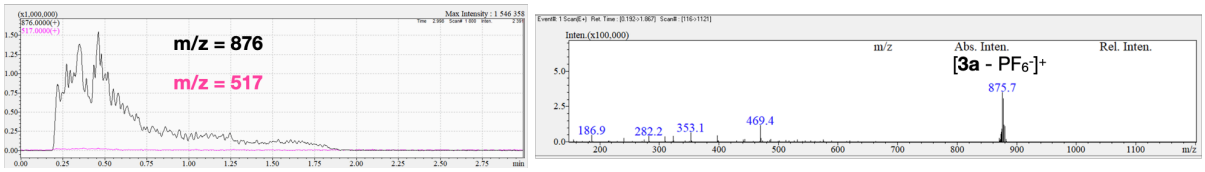

Supporting Figure S18. ESI-MS analysis of **3a** in DMSO solution after 0 and 24 h.

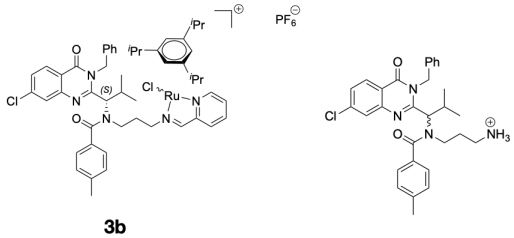

3b

m/z [**3b** - PF_6^-]$^+$

Chemical Formula: $C_{51}H_{60}Cl_2N_5O_2Ru^+$
Exact Mass: 946.3

m/z [**1**+H]$^+$

Chemical Formula: $C_{30}H_{34}ClN_4O_2^+$
Exact Mass: 517.2

ESI-MS Analysis of 3b in DMSO - direct injection

t = 0 min m/z extracted from TIC chromatogram

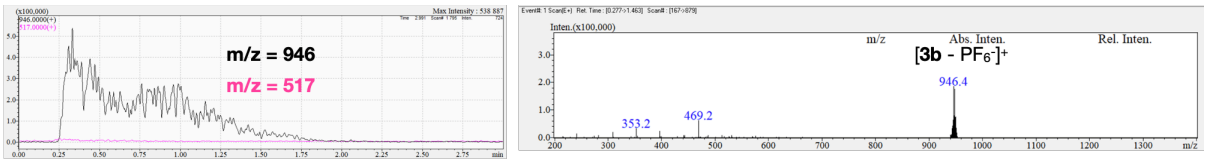

t = 24 h

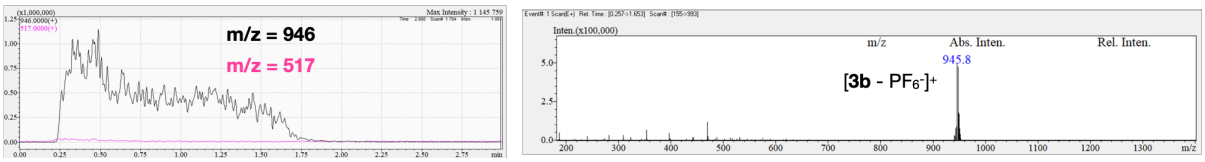

Supporting Figure S19. ESI-MS analysis of **3b** in DMSO solution after 0 and 24 h.

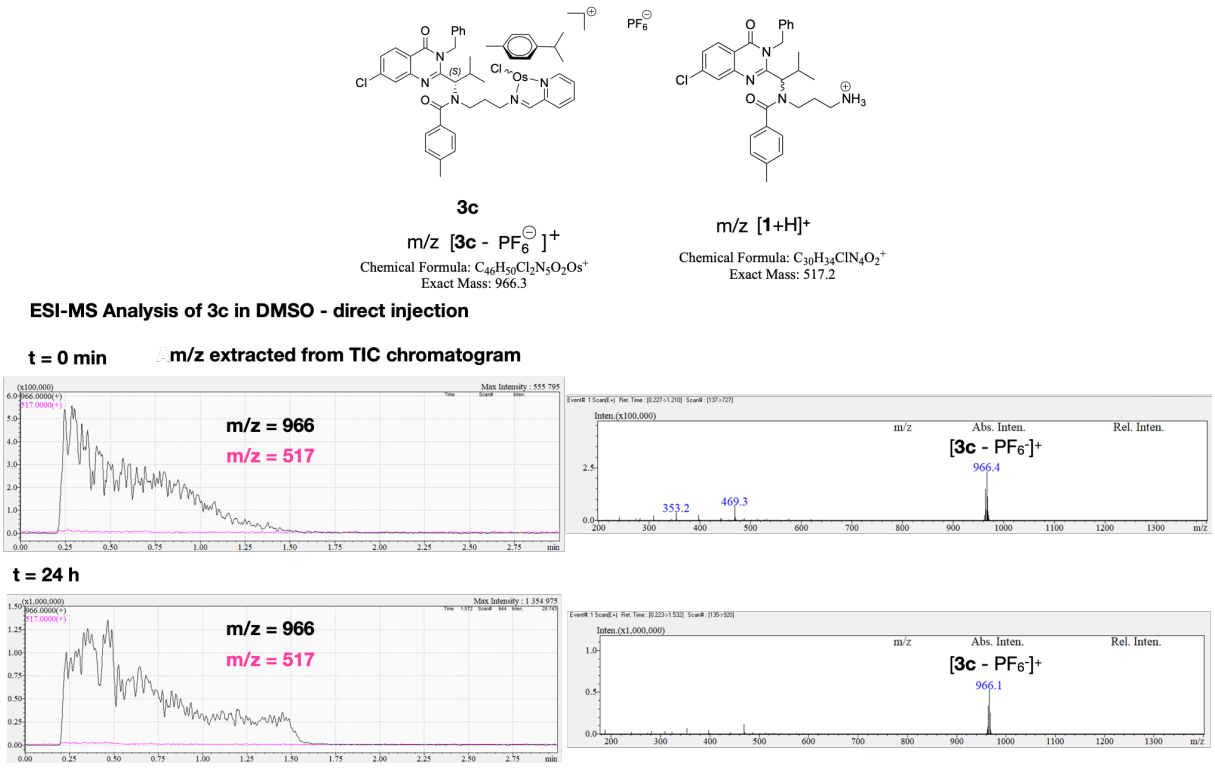

Supporting Figure S20. ESI-MS analysis of **3c** in DMSO solution after 0 and 24 h.

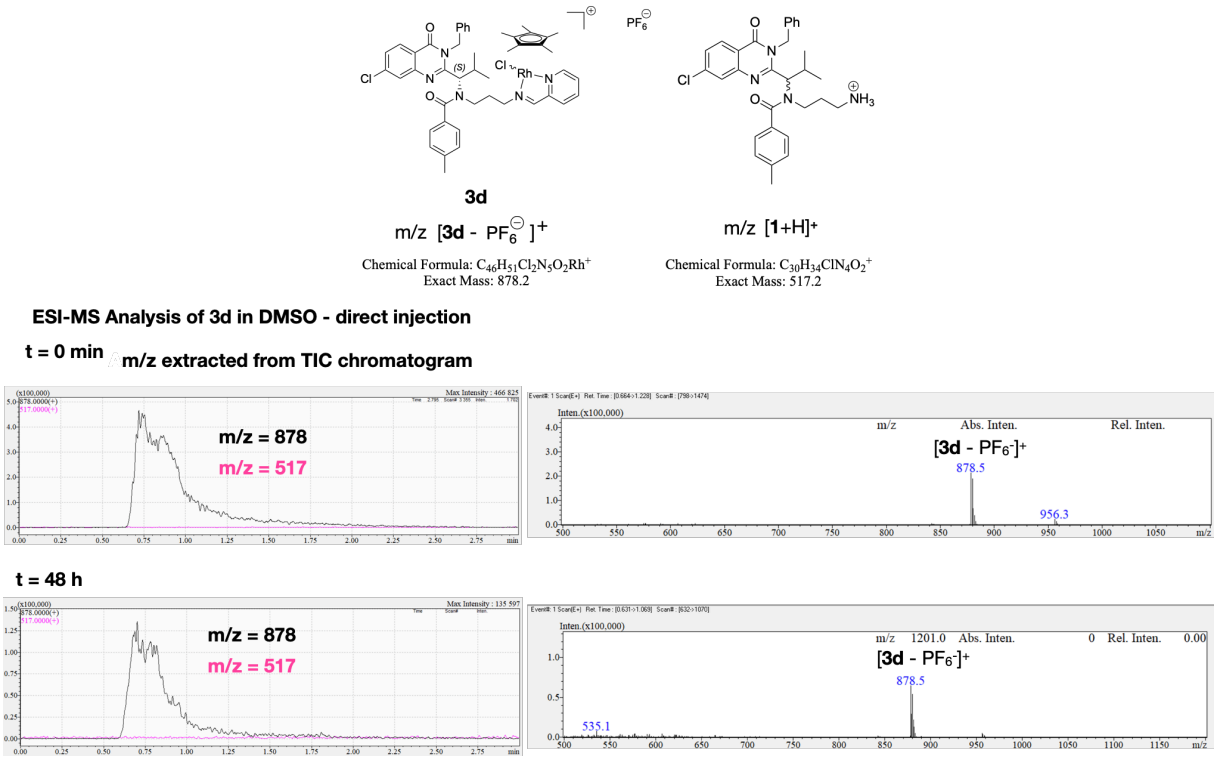

Supporting Figure S21. ESI-MS analysis of **3d** in DMSO solution after 0 and 48 h.

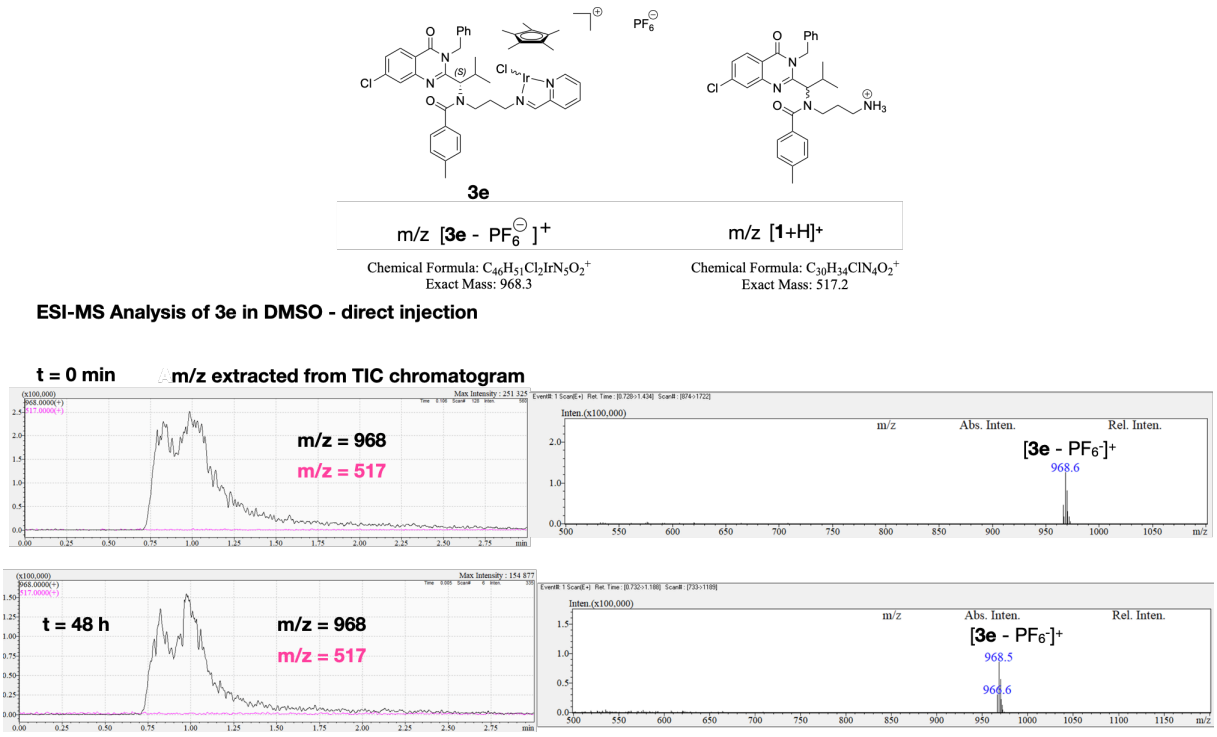

Supporting Figure S22. ESI-MS analysis of **3e** in DMSO solution after 0 and 48 h.

Stability in DMEM – UV-VIS analysis

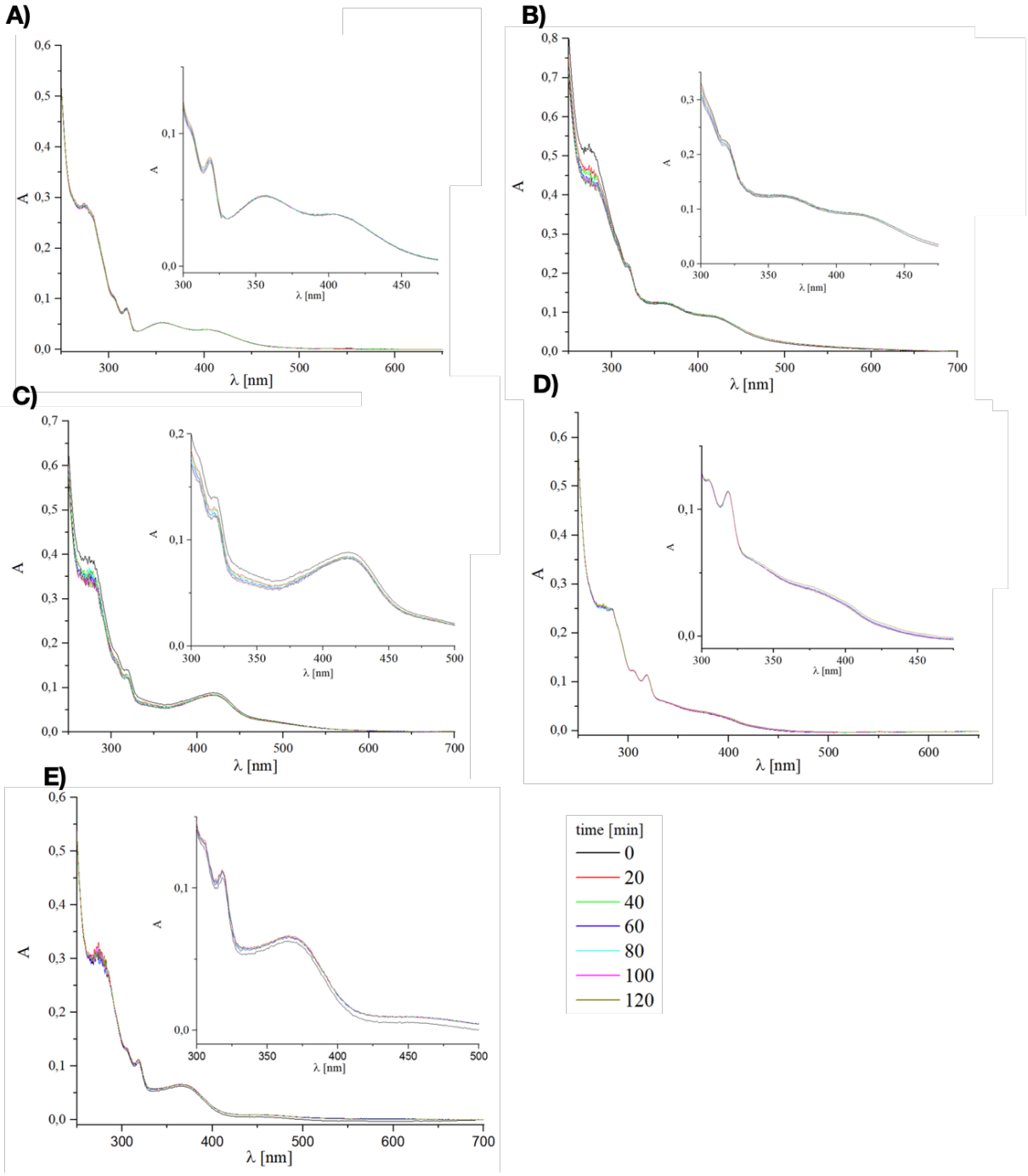

Supporting Figure S23. UV-VIS spectra of compounds **3a** (A), **3b** (B), **3c** (C), **3d** (D) and **3e** (E) in DMEM at c = 10 μM.

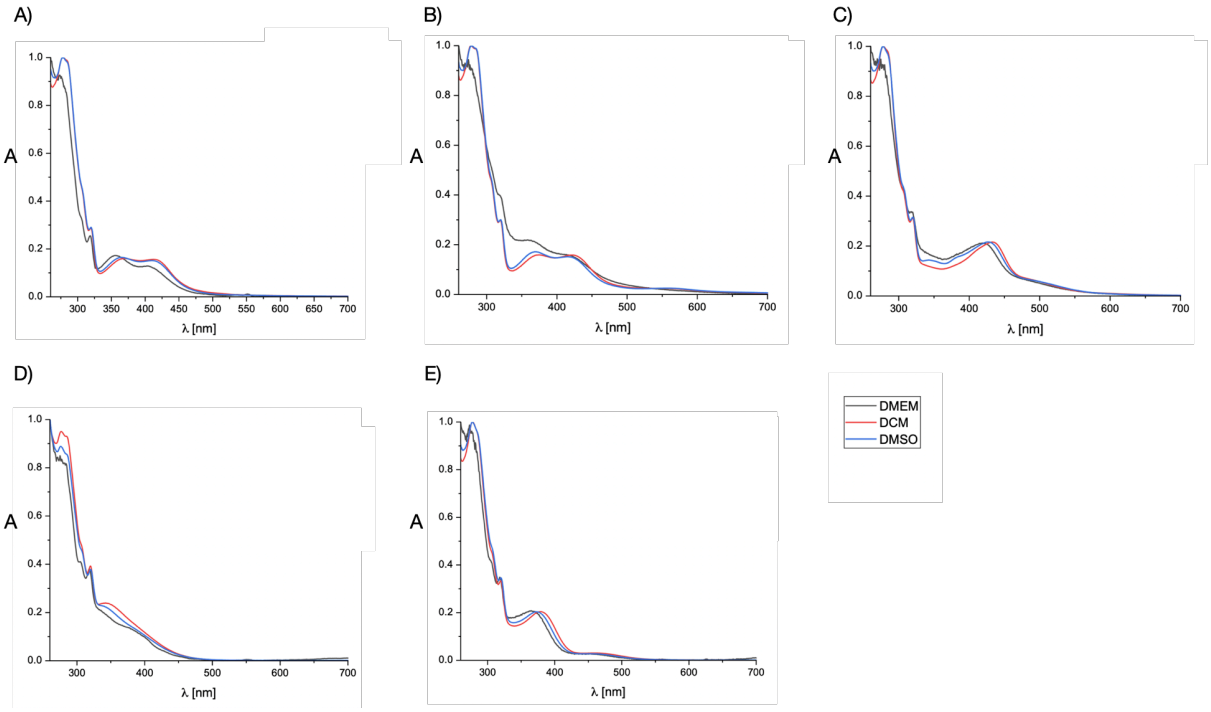

Supporting Figure S24. Normalized UV-VIS spectra of compounds **3a** (A), **3b** (B), **3c** (C), **3d** (D) and **3e** (E) in DMEM, DCM and DMSO.

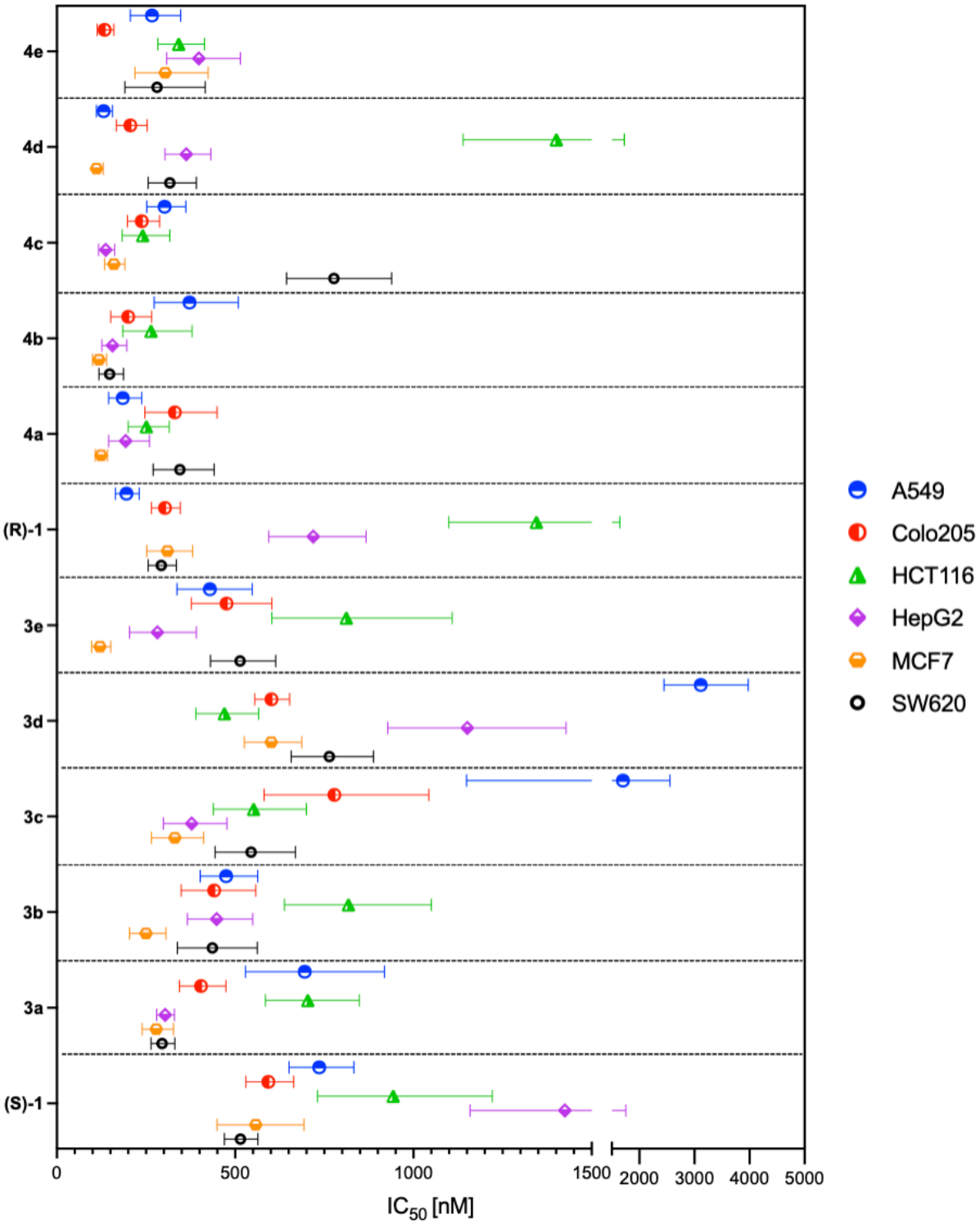

Supporting Figure S25. Graphical presentation of IC_{50} values of (S)-**1** and (*R*)-**1** derivatives obtained for investigated cancer cell lines. IC_{50} values are presented along with the corresponding 95% confidence intervals, n = 3;

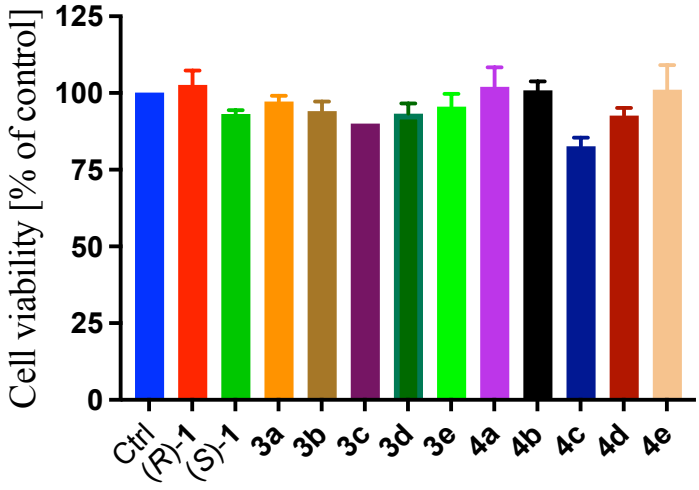

Supporting Figure S26. MRC-5 cells viability in the presence of compounds (*S*)- and (*R*)-**1** and **3a-4e** at concentrations equal to IC_{50} values determined for MCF-7 cells. Values are presented as mean ± SEM, n = 3;

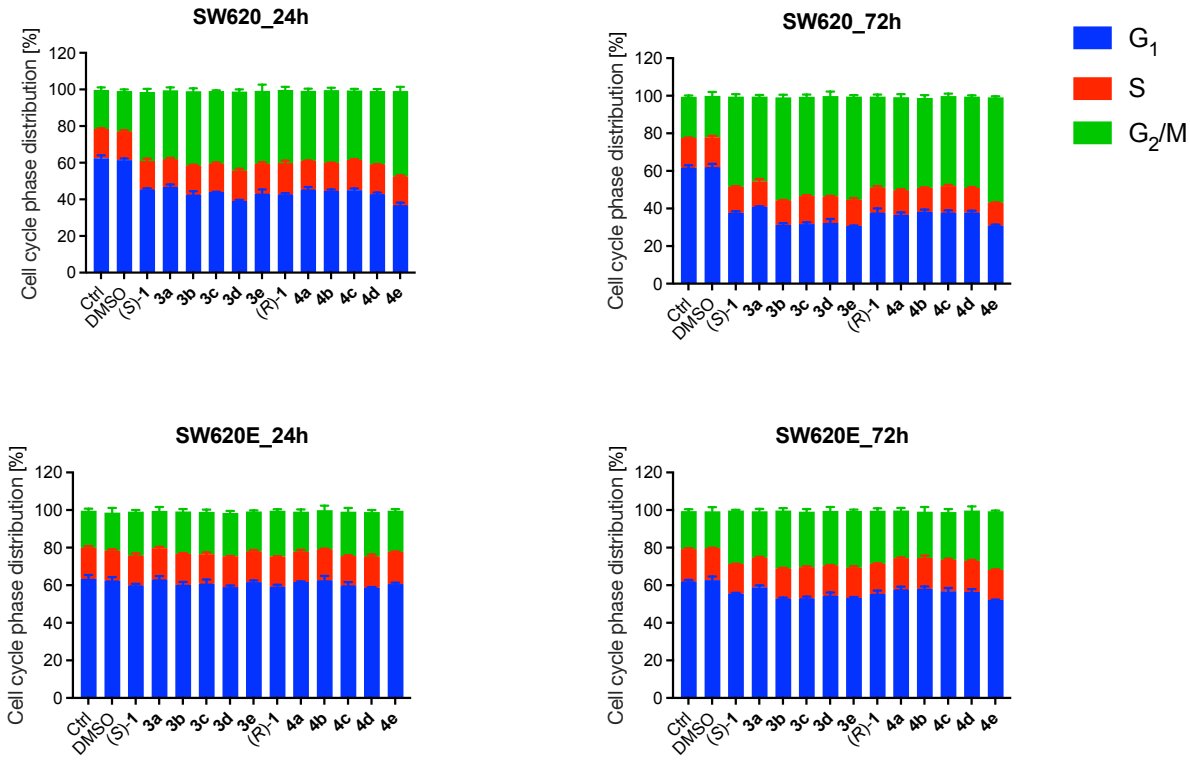

Figure S27. Cell cycle phase distribution for SW620 (top) and SW620E (bottom) cells exposed for 24 h and 72 h to (*S*)-**1** and (*R)*-**1** and the corresponding synthesized metal complexes **3a-4e** at concentrations equal to IC_{75} of (*S*)- and (*R)*-**1**, respectively. Data are presented as mean ± SEM, n = 3.

Molecular Modelling

The compounds were docked to the crystal structure of human kinesin KSP (PDB ID: 4AP0, resolution 2.59 Å)[1] which was obtained from the Protein Data Bank (PDB).[2, 3] Scigress version FJ 2.6[4] was used to prepare the crystal structure for docking, i.e., hydrogen atoms were added and the co-crystallized ispinesib and adenosine-5'-diphosphate (ADP) were removed. The center of the binding pocket was defined as the nitrogen in the ring close to the carbonyl group. (x = 41.663, y = 0.113, z = 11.931) with a radius of 10 Å. The GoldScore (GS),[5] ChemScore (CS)[6, 7], ChemPLP[8] and Astex statistical potential (ASP)[9] scoring functions were implemented to validate the predicted binding modes and relative energies of the compounds using the GOLD v5.4 software suite. The co-crystallized molecule ispinesib was first docked and root mean square deviation (RMSD) values were calculated for the heavy atoms. ASP obtained an average RMSD of 0.9255, the score for PLP was 0.7299, for CS 0.7265 and GS gave a RMSD of 0.8090 which show the strong prediction power of the scoring functions (Supporting Tables S2 and S3).

Supporting Table S2. RMSD values for heavy atoms between the co-crystallized ispinesib and the docked molecule.

Poses	**ASP**	**ChemPLP**	**CS**	**GS**
1	0.9569	0.5933	0.6412	1.0677
2	0.8536	0.8291	0.6083	0.4090
3	0.9660	0.7674	0.9299	0.9503
Mean	0.9255	0.7299	0.7265	0.8090

Supporting Table S3. Results of the scoring function for the docking of the compounds to KSP.

Compound	ASP	ChemPLP	ChemScore	GoldScore
ispinesib	48.7	109.6	42.6	83.4
(*R*)-**1a**	49.0	111.3	43.9	79.7
(*S*)-**1a**	40.0	87.3	37.1	70.8
3a^{S,R}*Ru*	33.0	89.5	38.0	63.2
3a^{S,S}*Ru*	35.1	84.9	34.3	74.3
3c^{S,R}*Os*	38.3	92.9	38.8	62.8
3c^{S,S}*Os*	35.7	89.4	34.3	59.4
3d^{S,S}*Rh*	39.8	90.6	35.2	73.8
3d^{S,R}*Rh*	40.1	83.1	35.6	56.1
3e^{S,S}*Ir*	38.8	90.6	36.6	75.4
3e^{S,R}*Ir*	40.5	88.3	38.8	54.8
4a^{R,S}*Ru*	41.4	90.4	35.5	79.3
4a^{R,R}*Ru*	39.6	91.0	36.9	75.6
4c^{R,S}*Os*	40.2	95.2	37.0	67.7
4c^{R,R}*Os*	39.7	93.4	37.9	65.0
4d^{R,R}*Rh*	36.3	81.9	36.1	68.1
4d^{R,S}*Rh*	37.5	87.2	35.7	64.4
4e^{R,R}*Ir*	38.5	84.8	34.6	68.2
4e^{R,S}*Ir*	38.8	87.5	34.3	64.9

Copies of NMR spectra

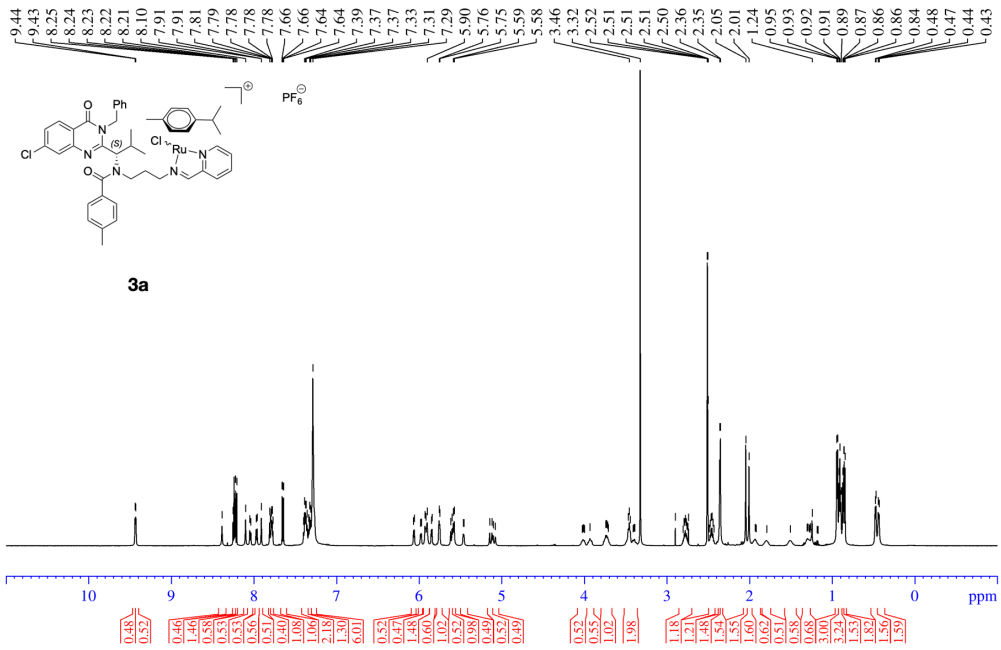

Supporting Figure S28. ^{1}H NMR of **3a** in DMSO-d_6

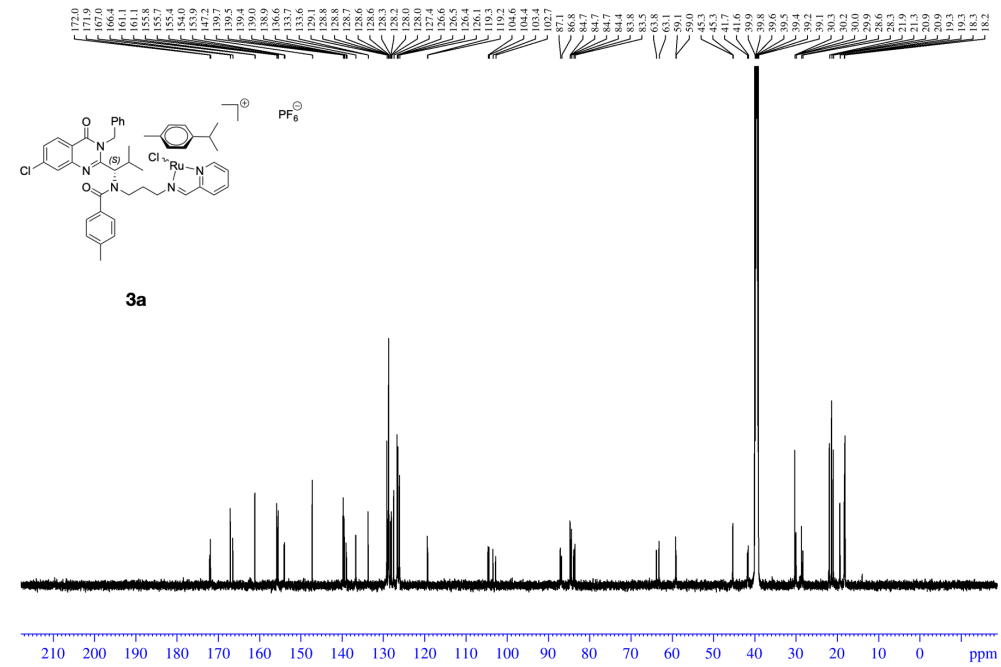

Supporting Figure S29. $^{13}C\{^{1}H\}$ NMR of **3a** in DMSO-d_6

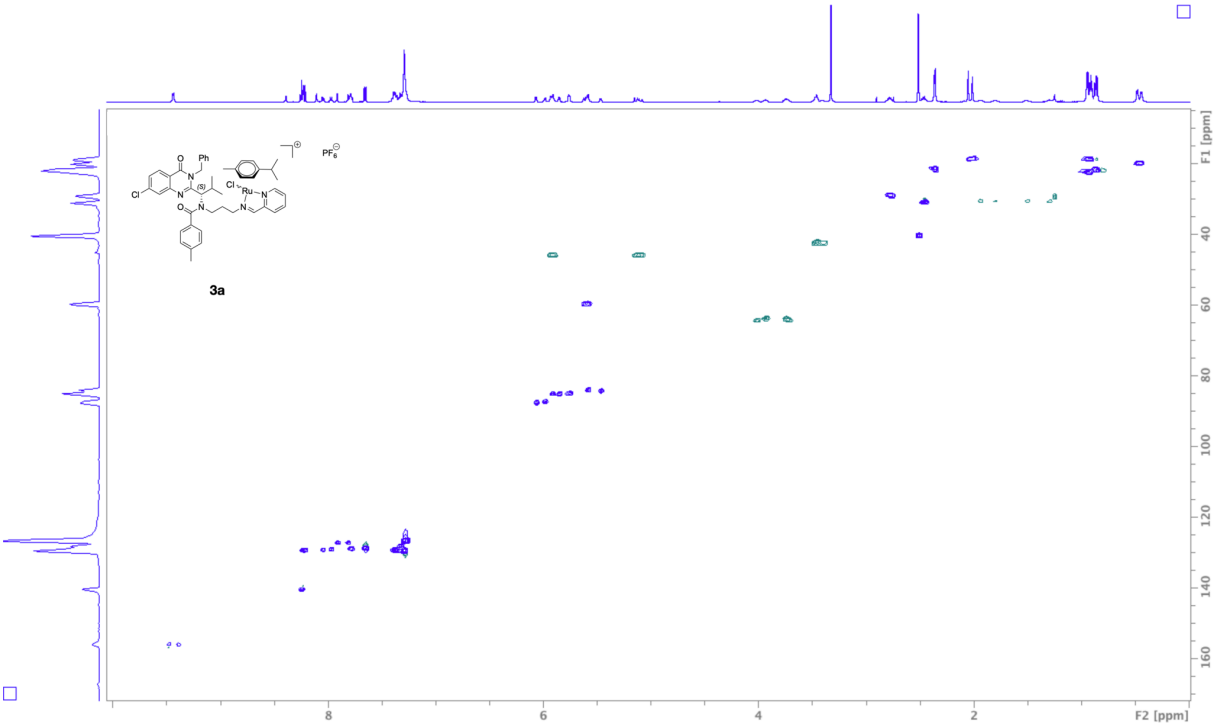

Supporting Figure S30. ^{1}H-^{13}C HSQC NMR of **3a** in DMSO-d$_6$

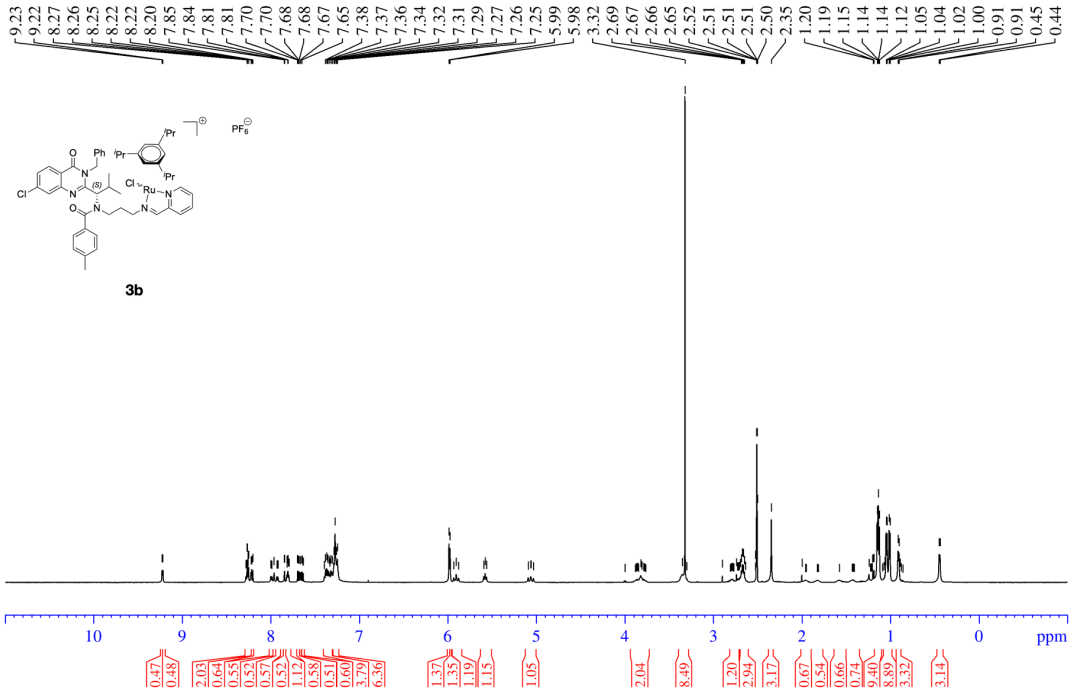

Supporting Figure S31. ^{1}H NMR of **3b** in DMSO-d$_6$

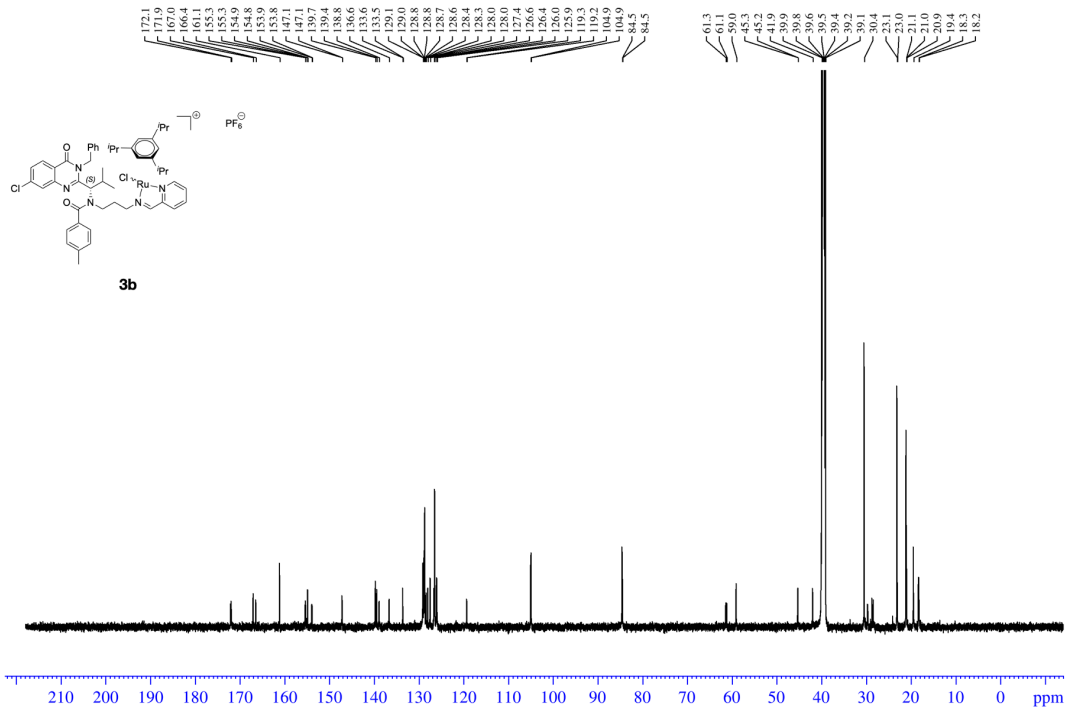

Supporting Figure S32. $^{13}C\{^{1}H\}$ NMR of **3b** in DMSO-d_6

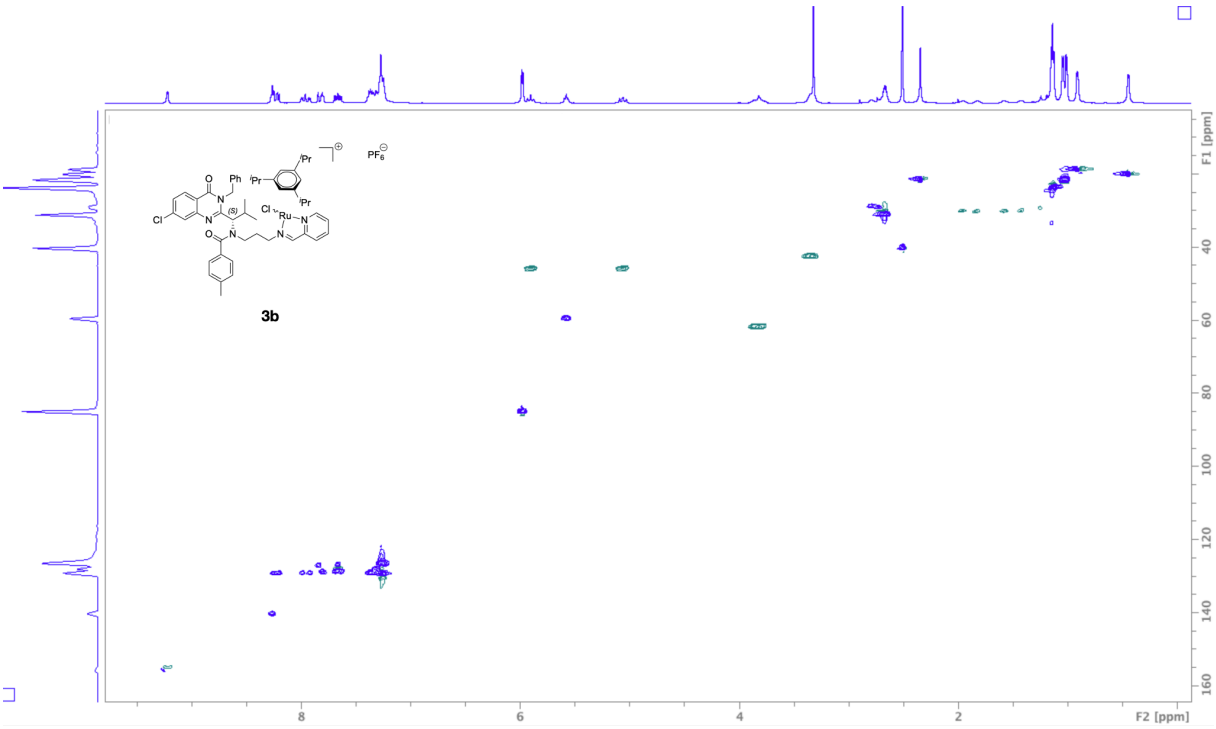

Supporting Figure S33. ^{1}H-^{13}C HSQC NMR of **3b** in CD_2Cl_2

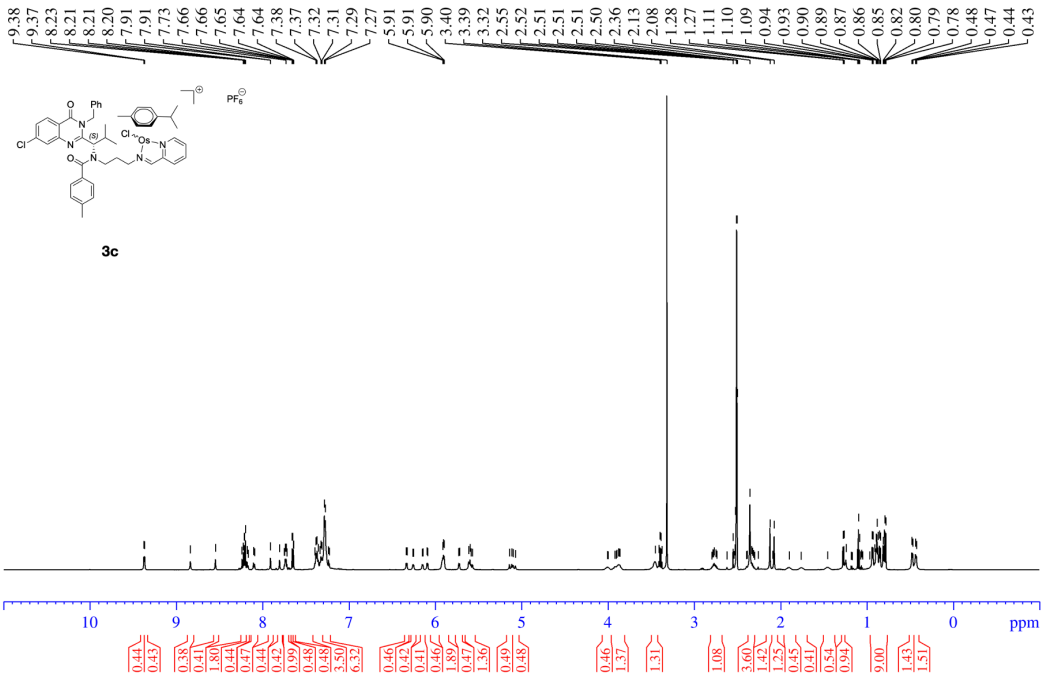

Supporting Figure S34. ^{1}H NMR of **3c** in DMSO-d_6

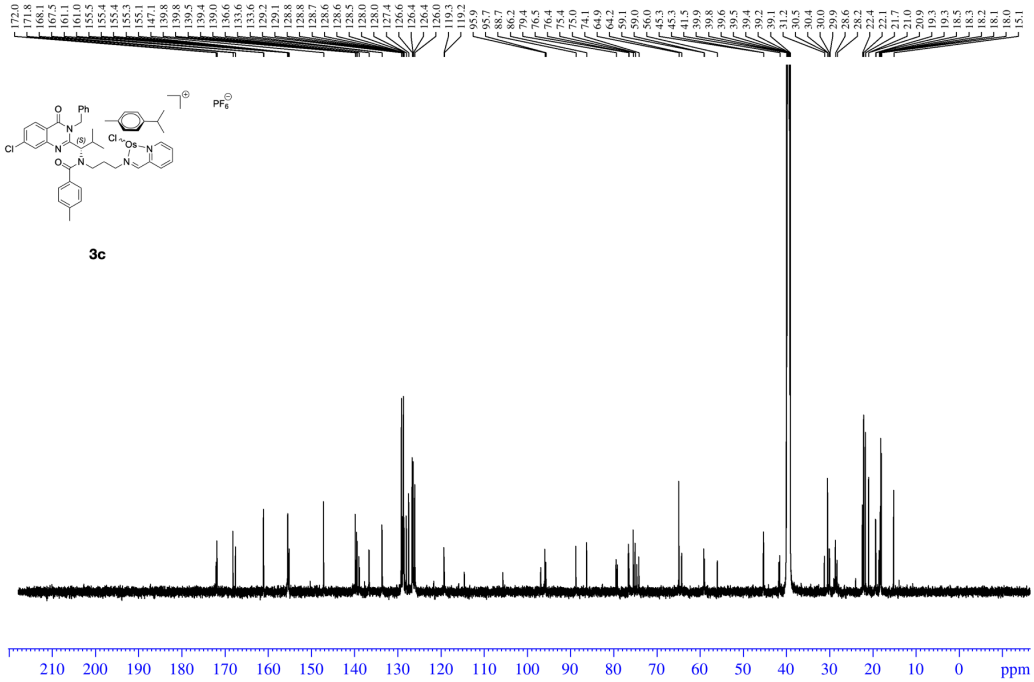

Supporting Figure S35. $^{13}C\{^{1}H\}$ NMR of **3c** in DMSO-d_6

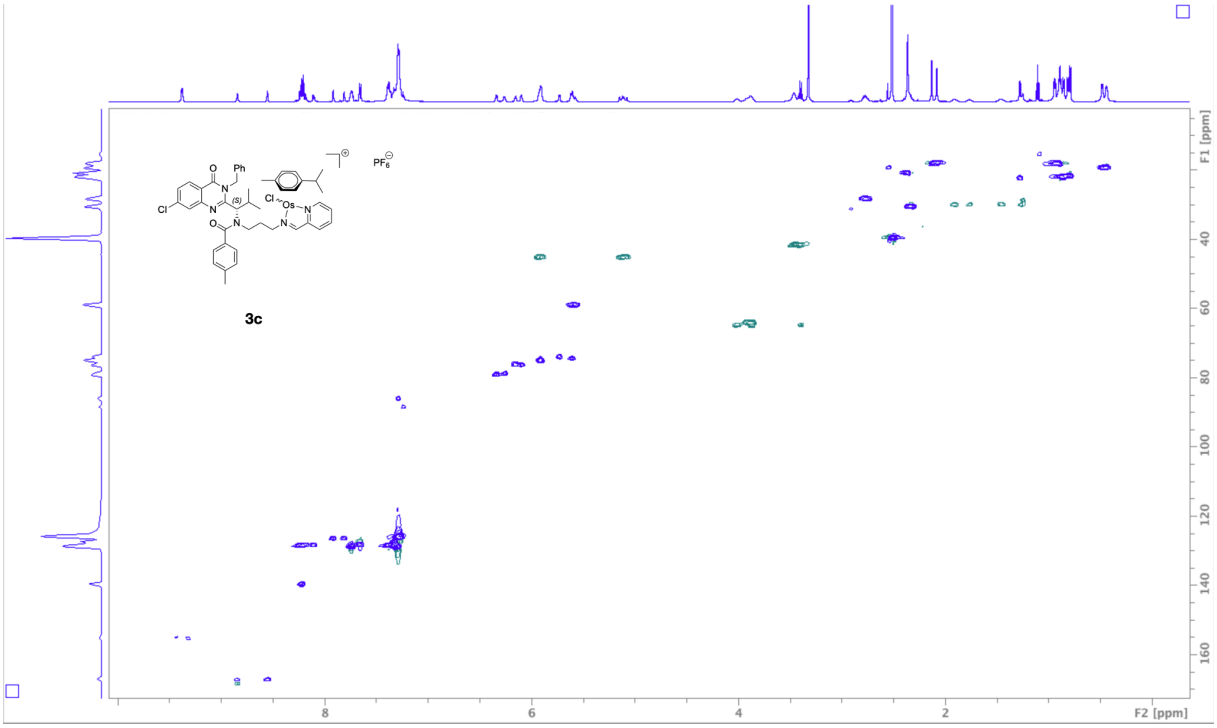

Supporting Figure S36. ^{1}H-^{13}C HSQC NMR of **3c** in DMSO-d_6

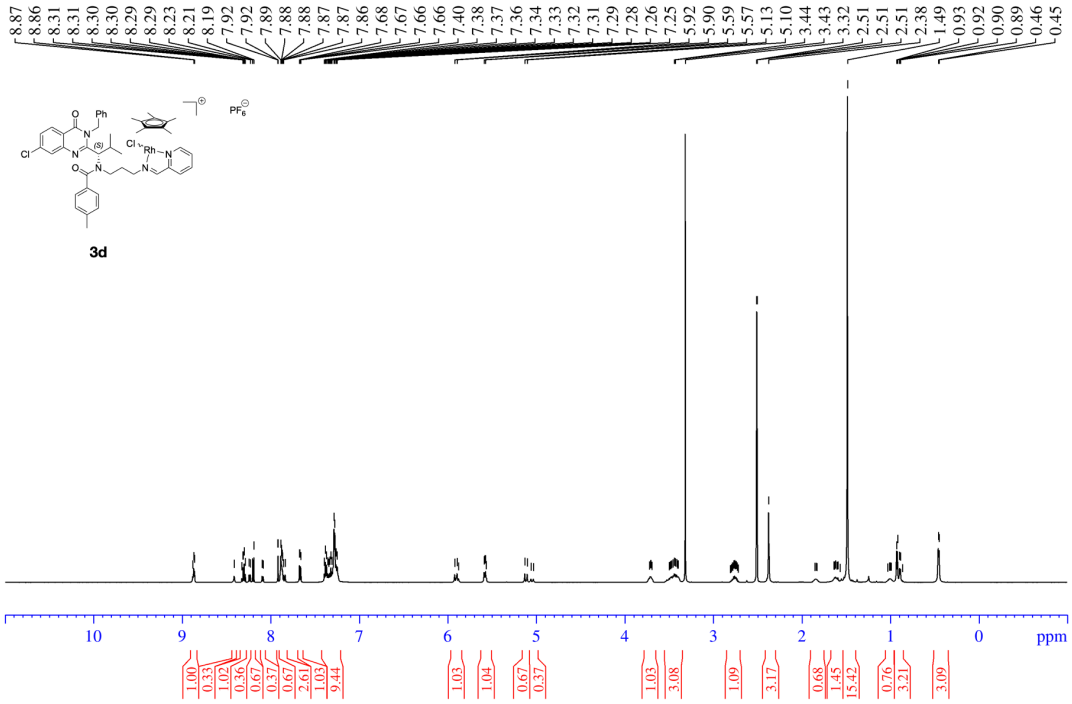

Supporting Figure S37. ^{1}H NMR of **3d** in DMSO-d_6

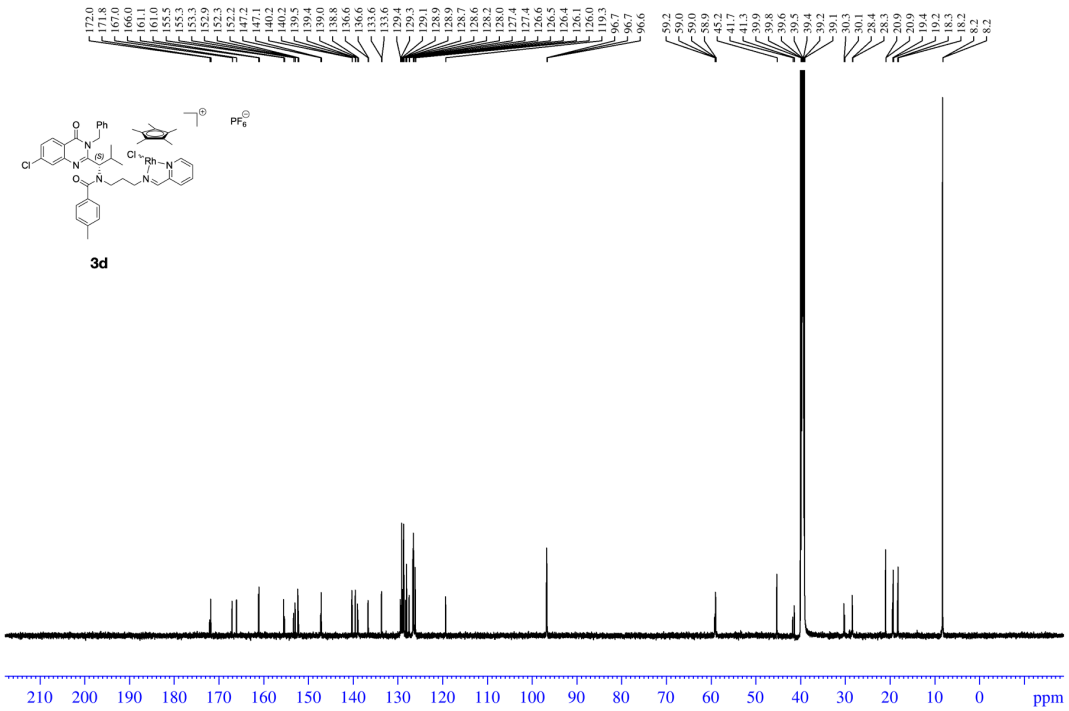

Supporting Figure S38. $^{13}C\{^{1}H\}$ NMR of **3d** in DMSO-d_6

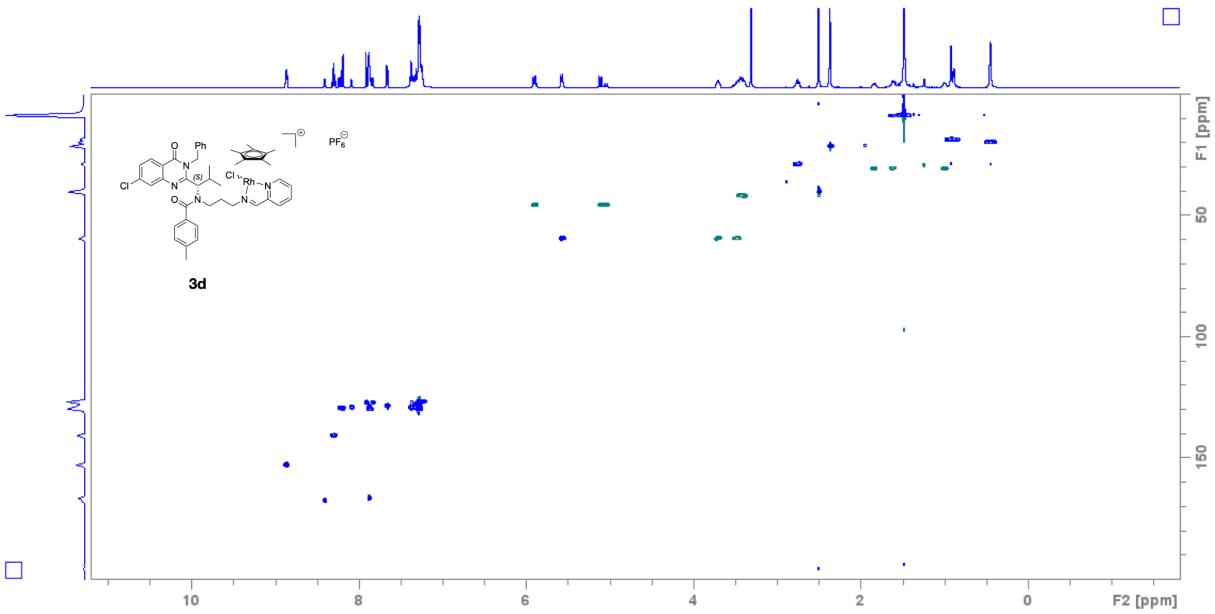

Supporting Figure S39. ^{1}H-^{13}C HSQC NMR of **3d** in DMSO-d_6

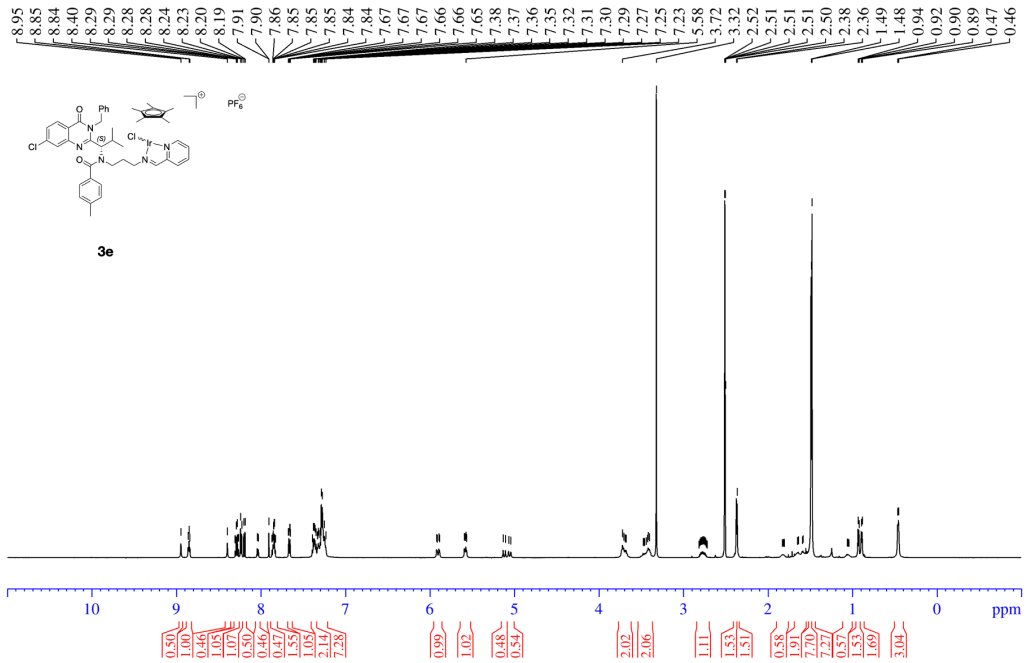

Supporting Figure S40. ^{1}H NMR of **3e** in DMSO-d_6

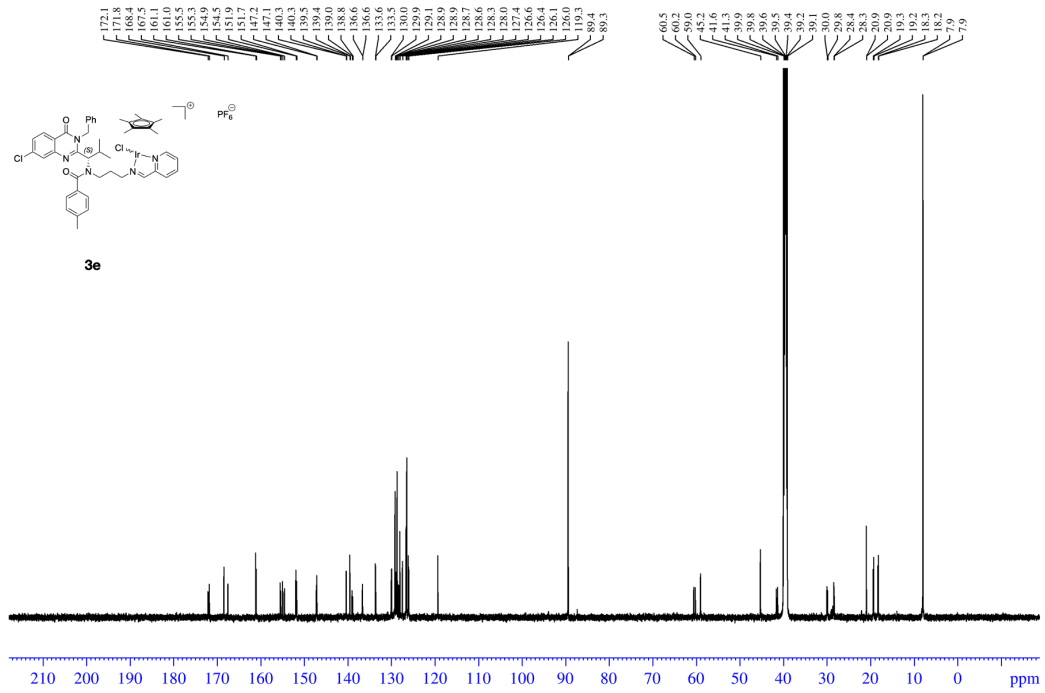

Supporting Figure S41. $^{13}C\{^{1}H\}$ NMR of **3e** in DMSO-d_6

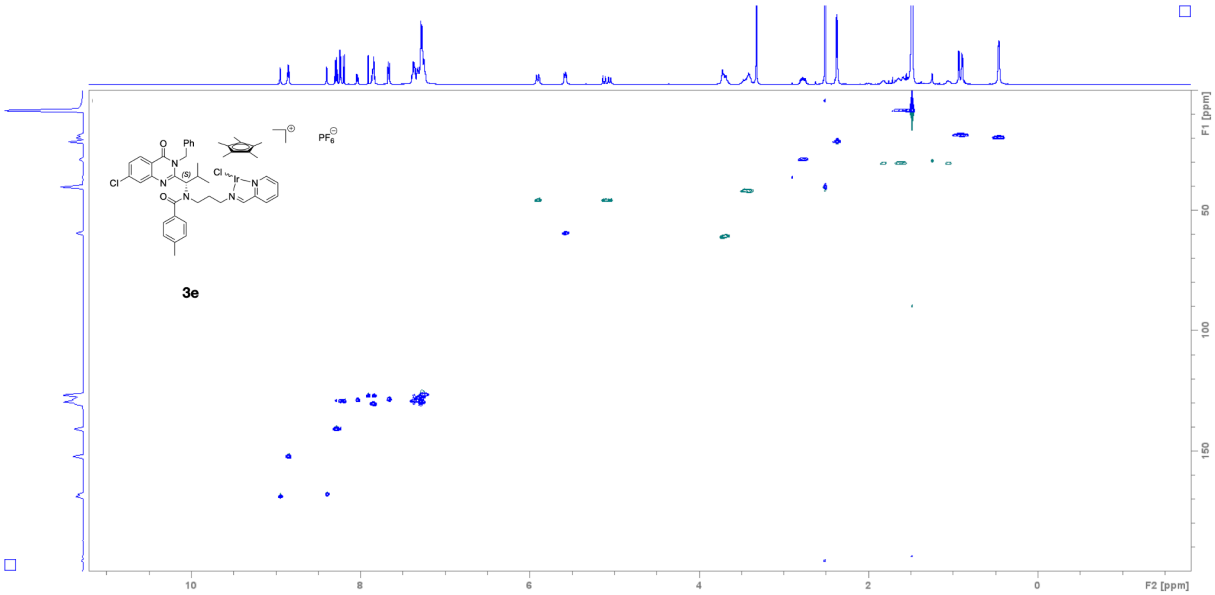

Supporting Figure S42. ^{1}H-^{13}C HSQC NMR of **3e** in DMSO-d_6

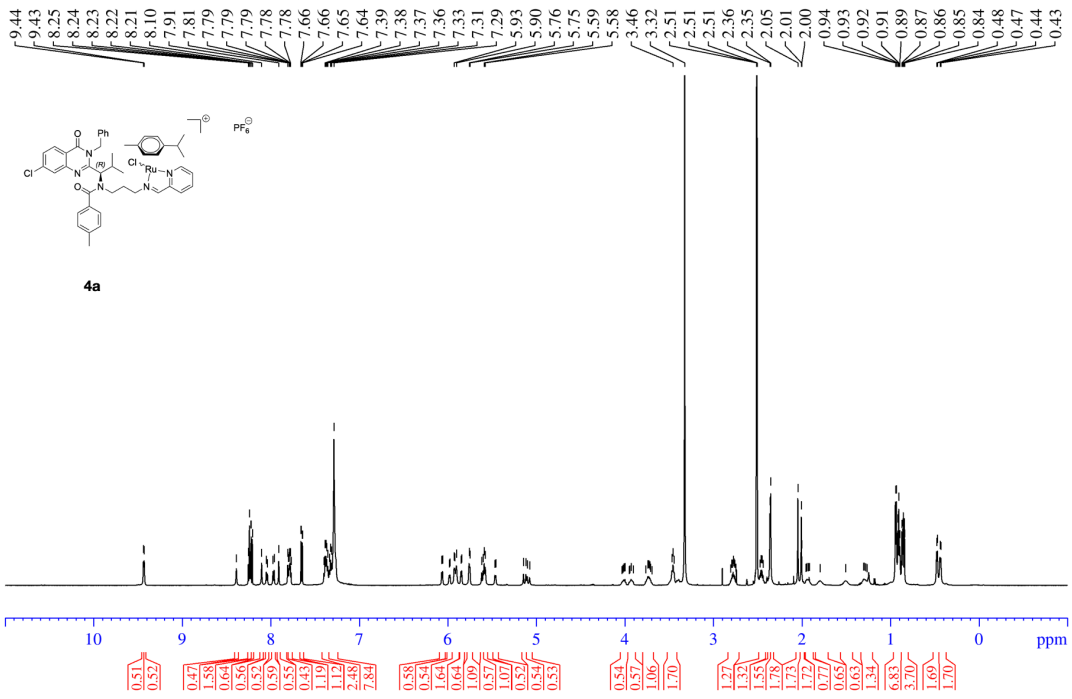

Supporting Figure S43. ^{1}H NMR of **4a** in DMSO-d_6

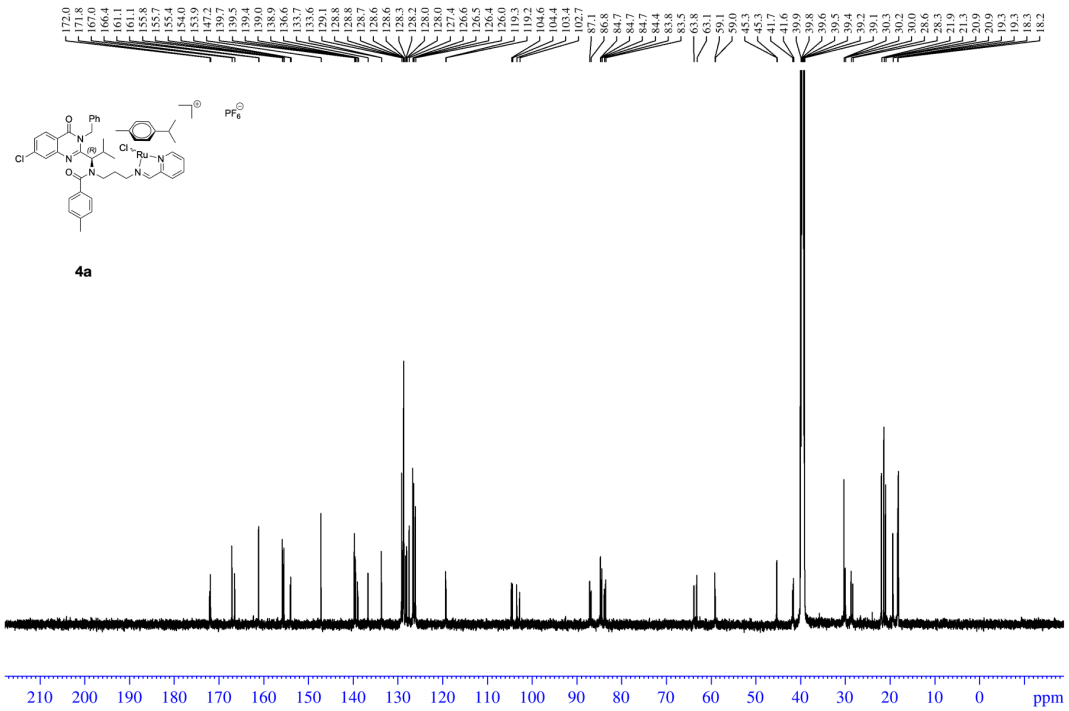

Supporting Figure S44. $^{13}C\{^{1}H\}$ NMR of **4a** in DMSO-d_6

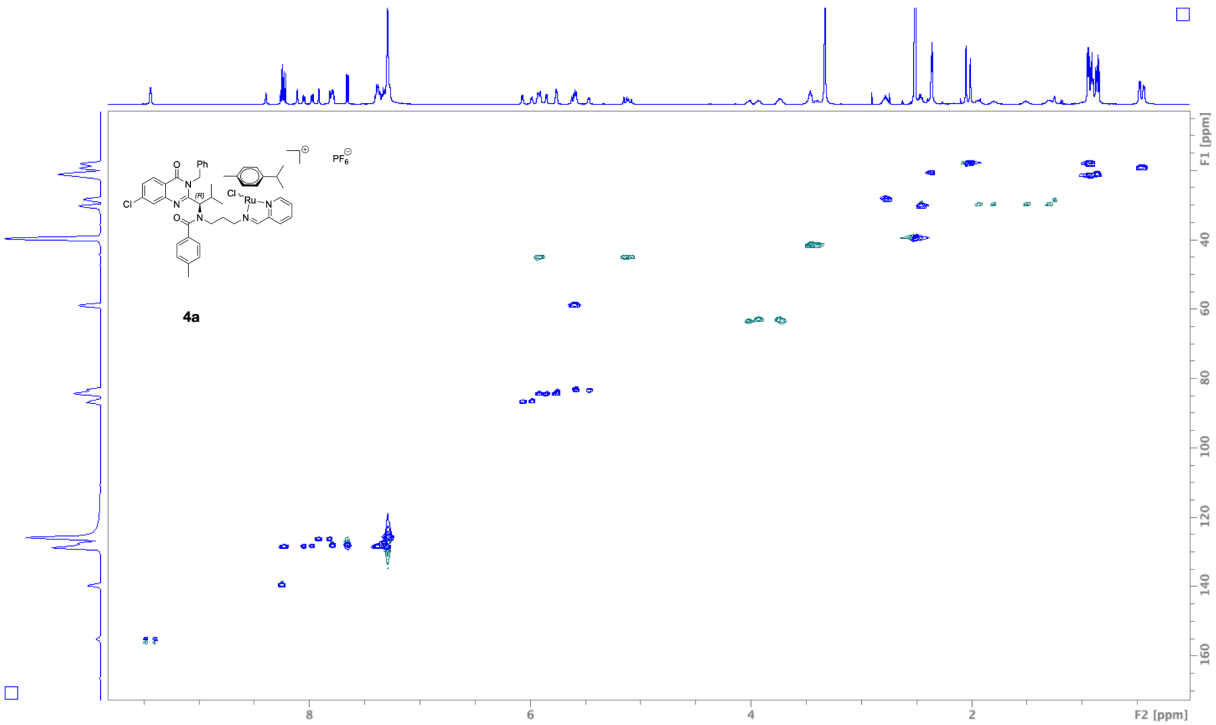

Supporting Figure S45. ^{1}H-^{13}C HSQC NMR of **4a** in DMSO-d_6

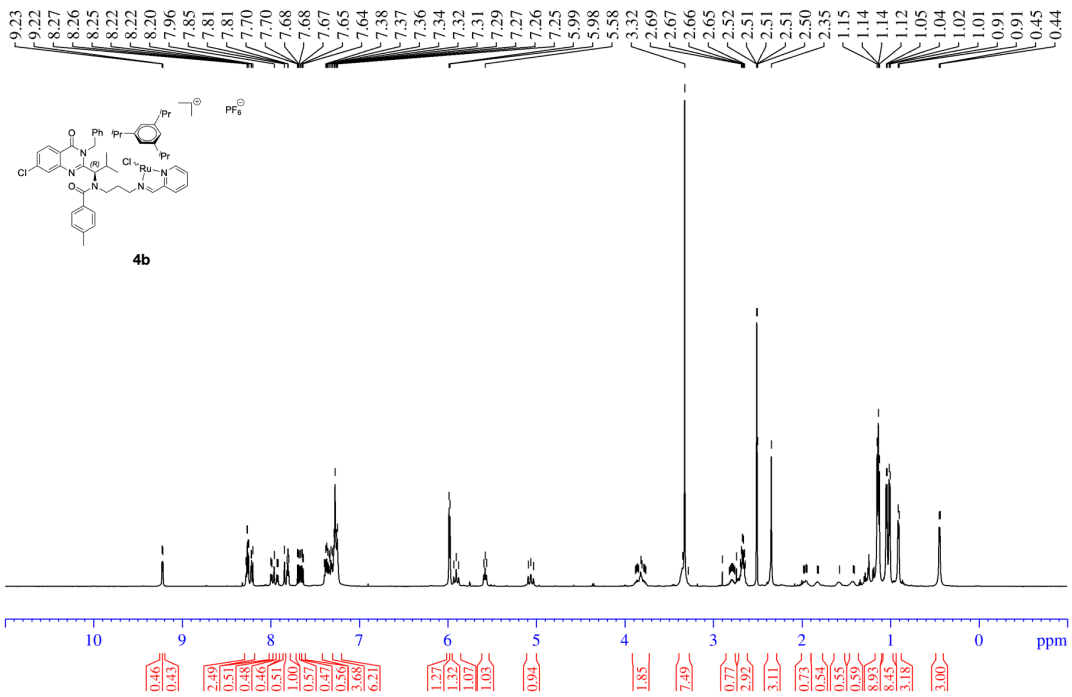

Supporting Figure S46. ^{1}H NMR of **4b** in DMSO-d_6

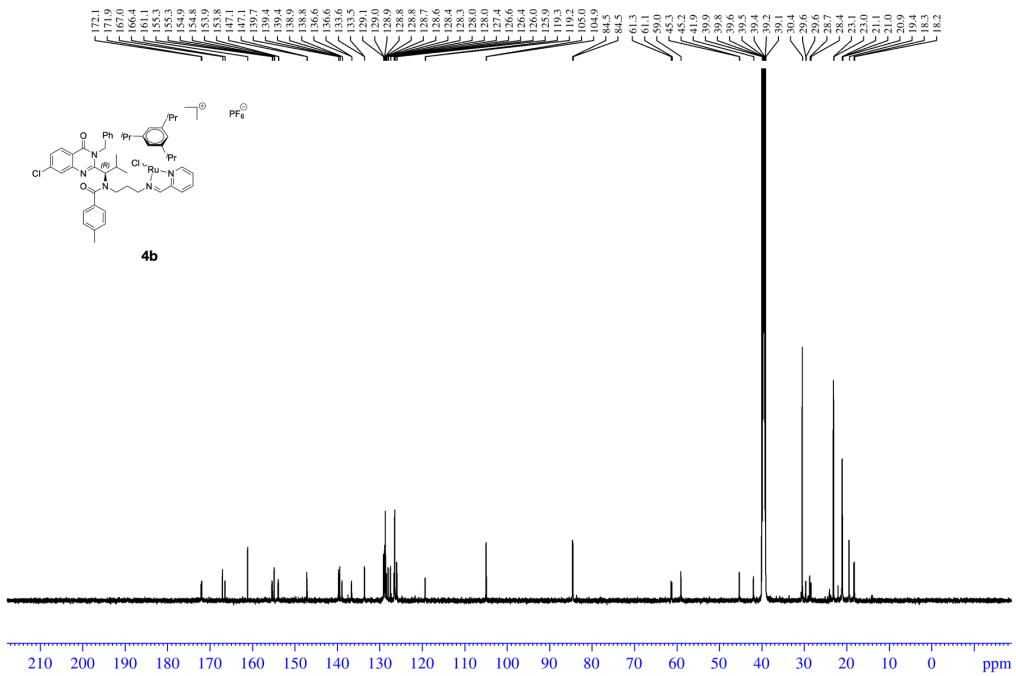

Supporting Figure S47. $^{13}C\{^{1}H\}$ NMR of **4b** in DMSO-d_6

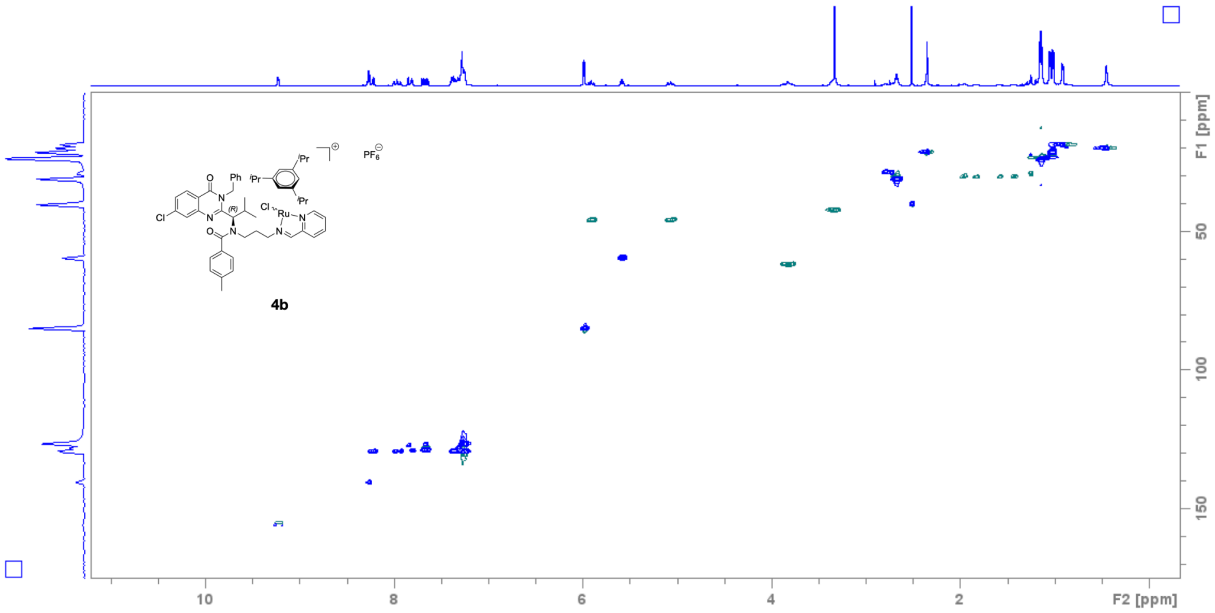

Supporting Figure S48. ^{1}H-^{13}C HSQC NMR of **4b** in DMSO-d_6

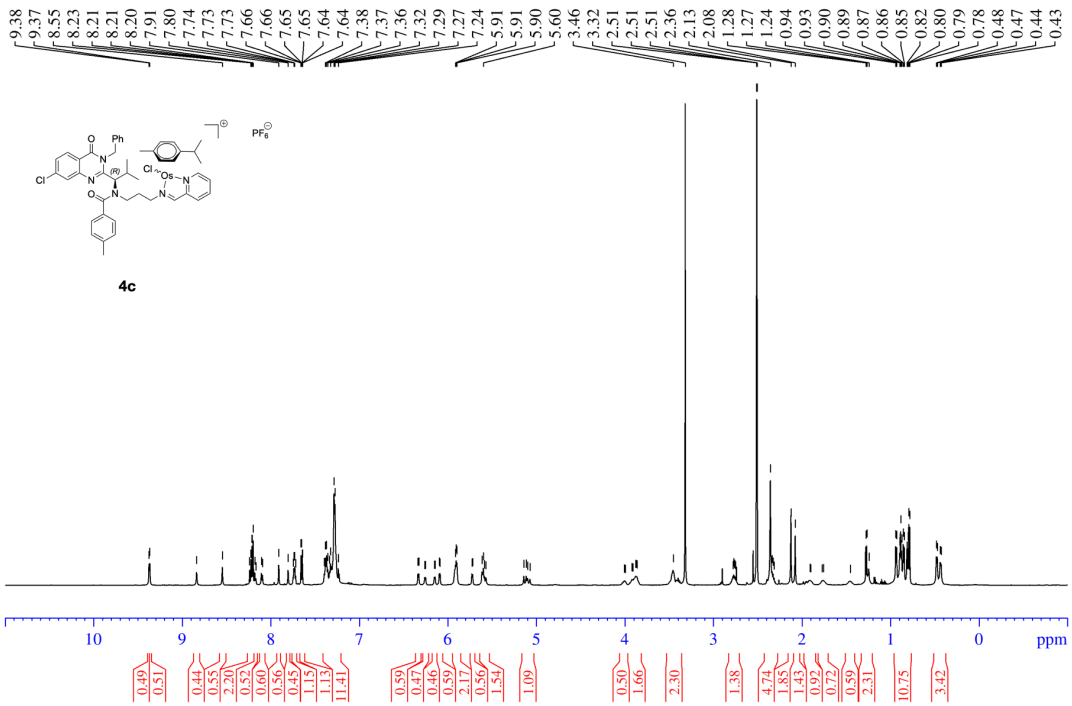

Supporting Figure S49. ^{1}H NMR of **4c** in DMSO-d_6

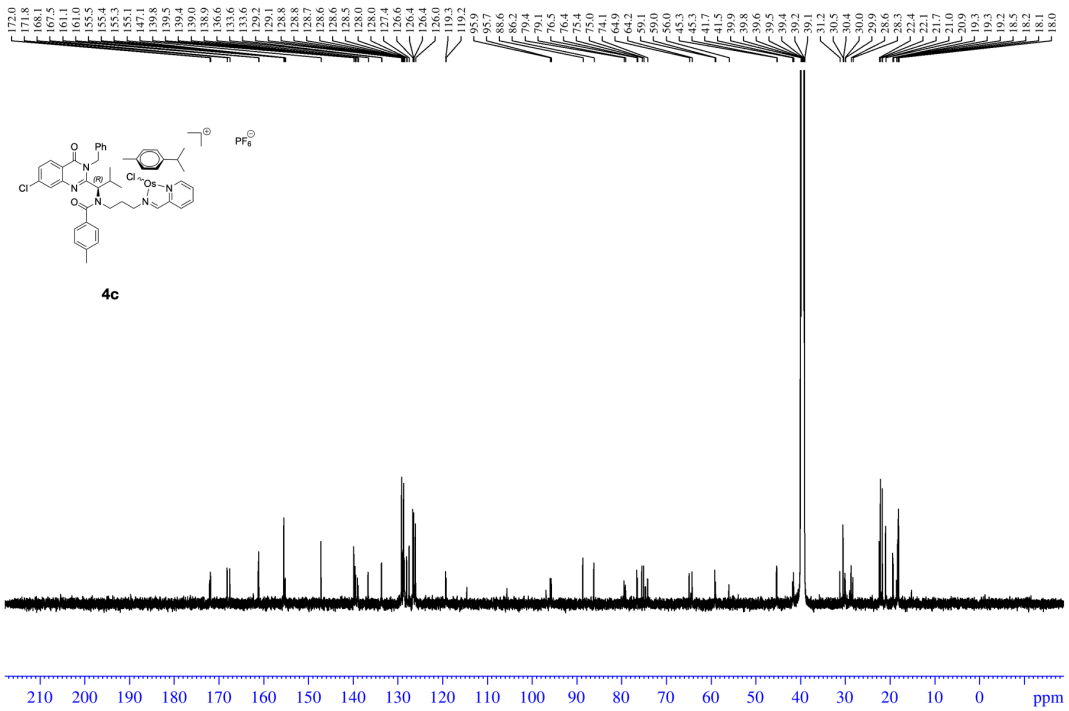

Supporting Figure S50. $^{13}C\{^{1}H\}$ NMR of **4c** in DMSO-d_6

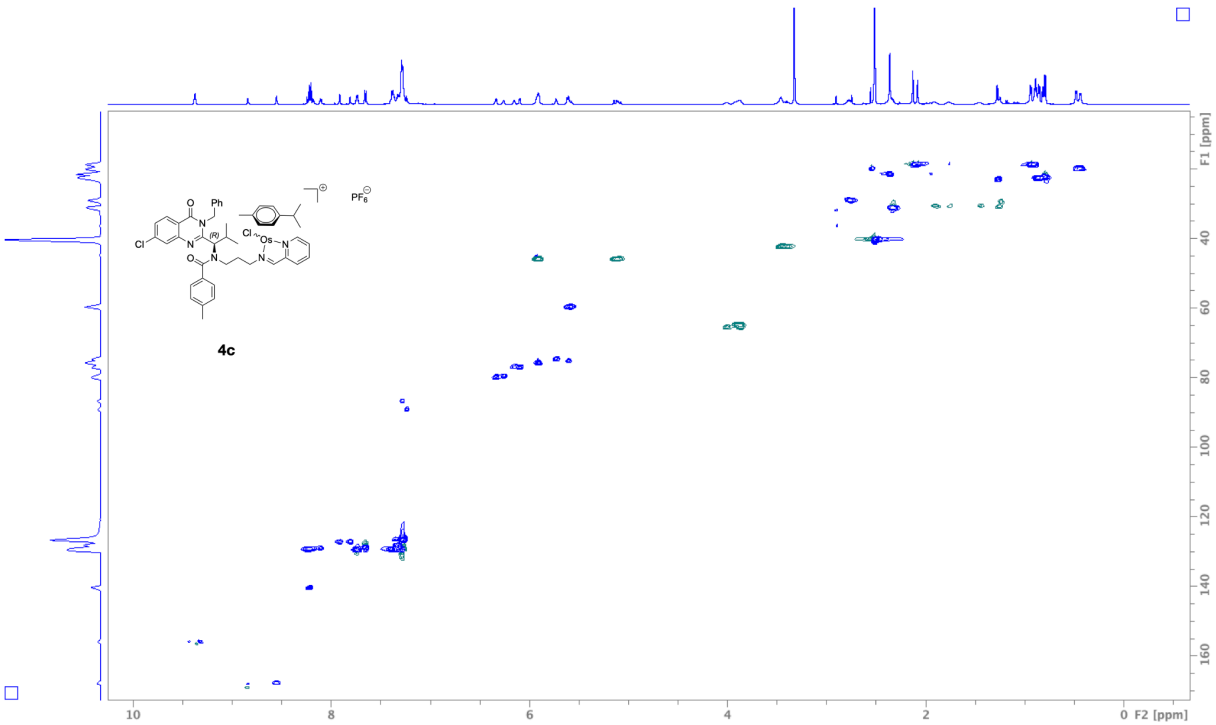

Supporting Figure S51. ^{1}H-^{13}C HSQC NMR of **4c** in DMSO-d_6

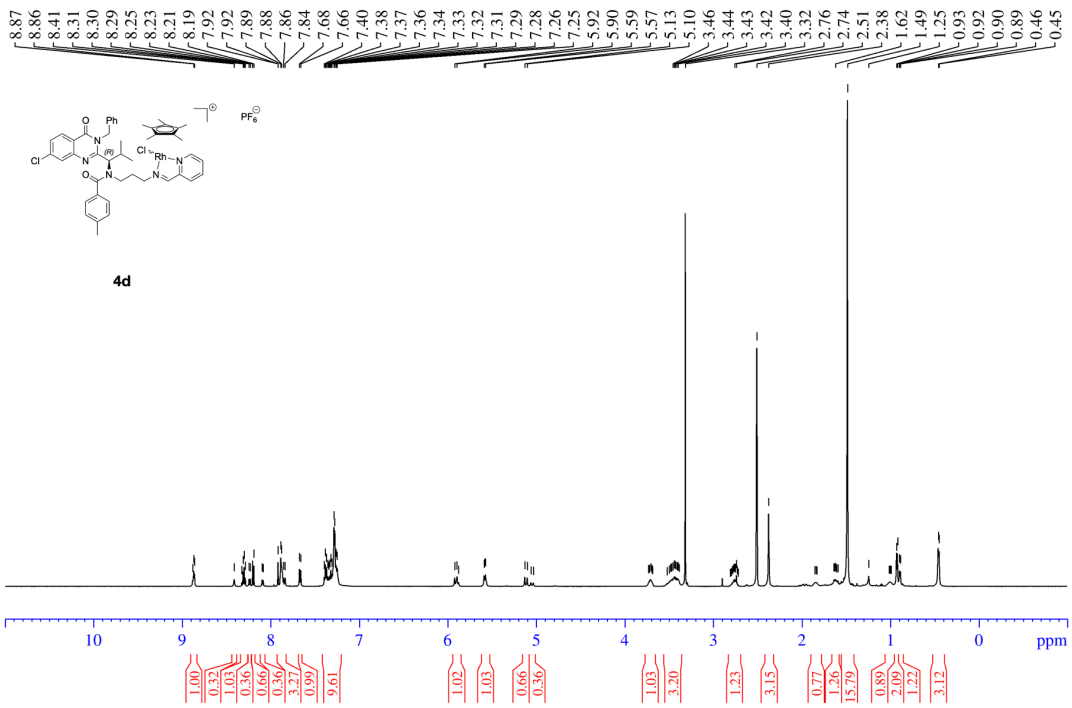

Supporting Figure S52. ^{1}H NMR of **4d** in DMSO-d_6

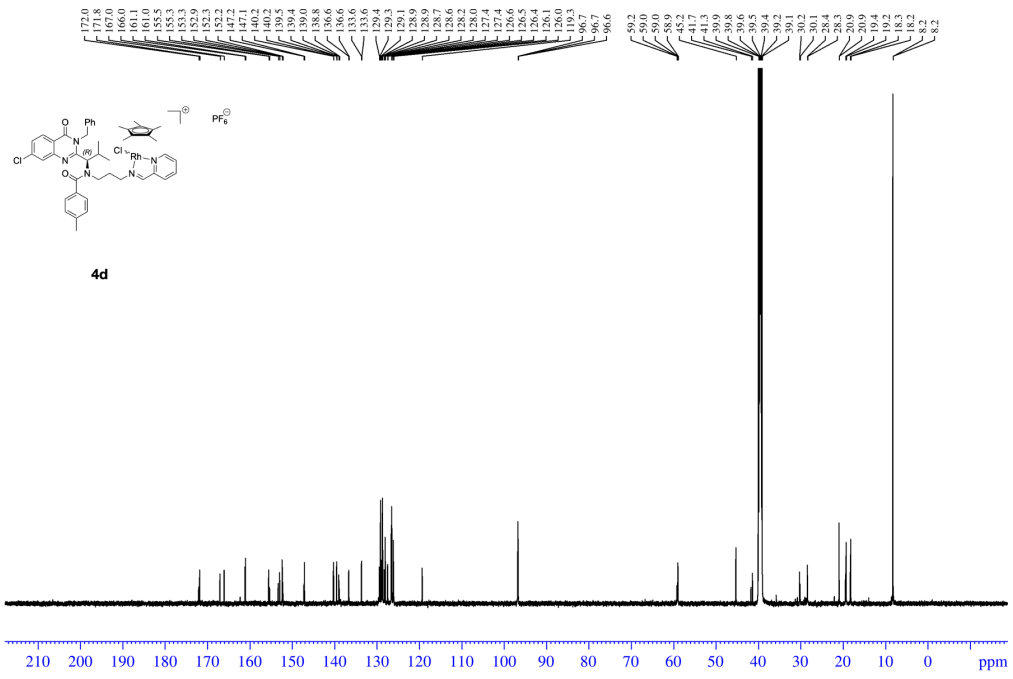

Supporting Figure S53. $^{13}C\{^{1}H\}$ NMR of **4d** in DMSO-d_6

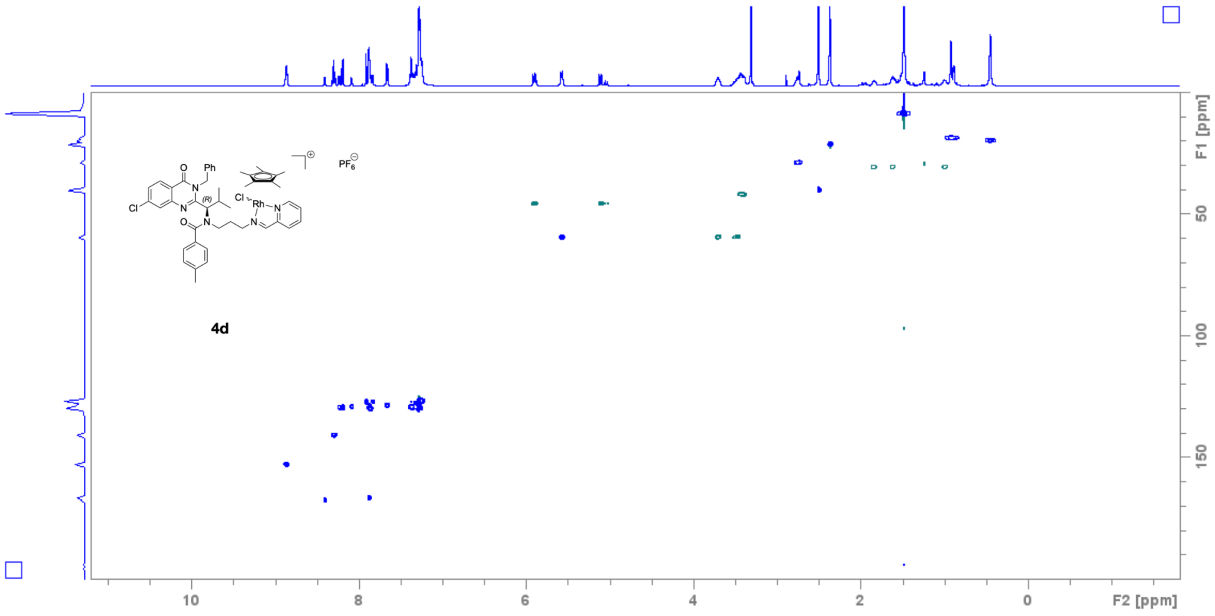

Supporting Figure S54. ^{1}H-^{13}C HSQC NMR of **4d** in DMSO-d_6

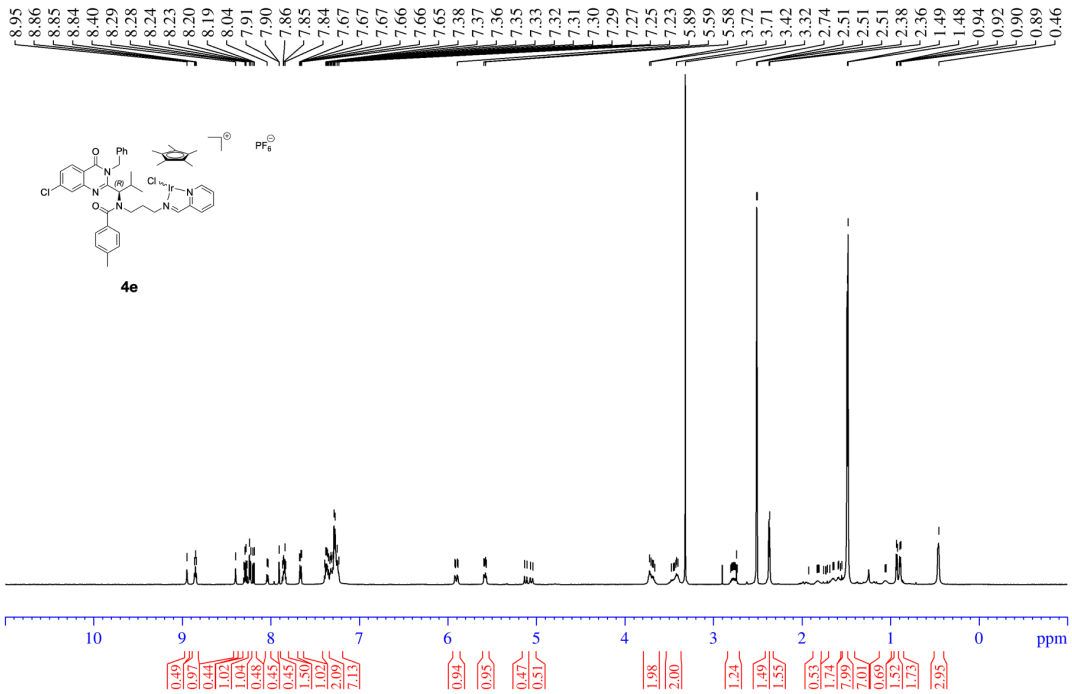

Supporting Figure S55. ^{1}H NMR of **4e** in DMSO-d_6

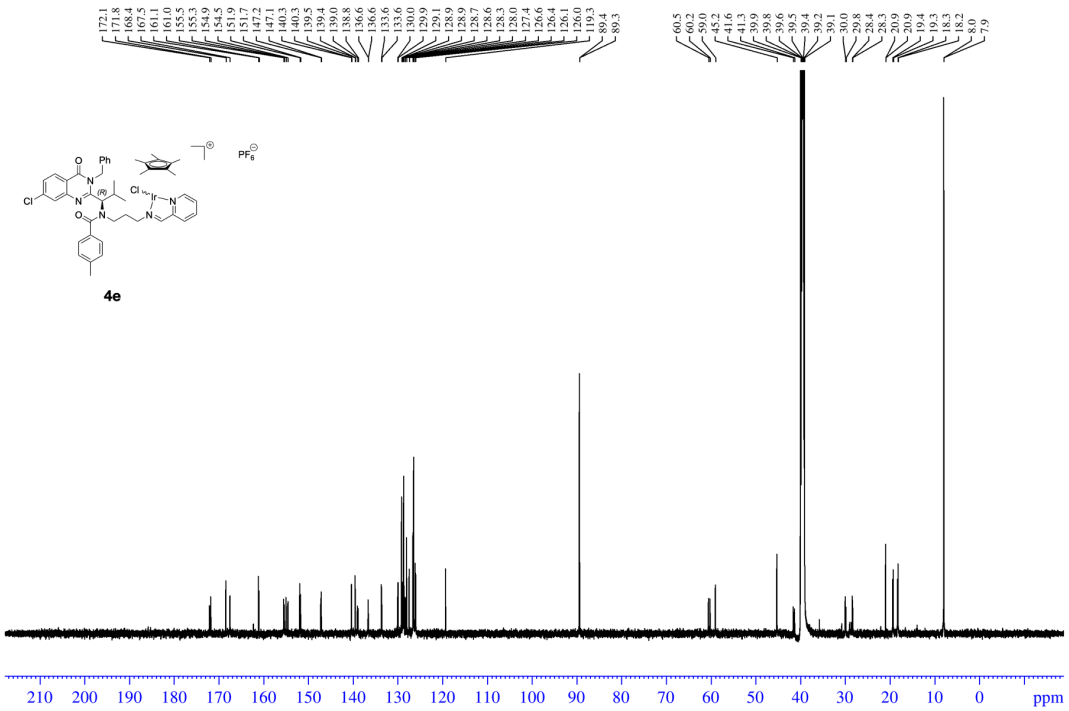

Supporting Figure S56. $^{13}C\{^{1}H\}$ NMR of **4e** in DMSO-d_6

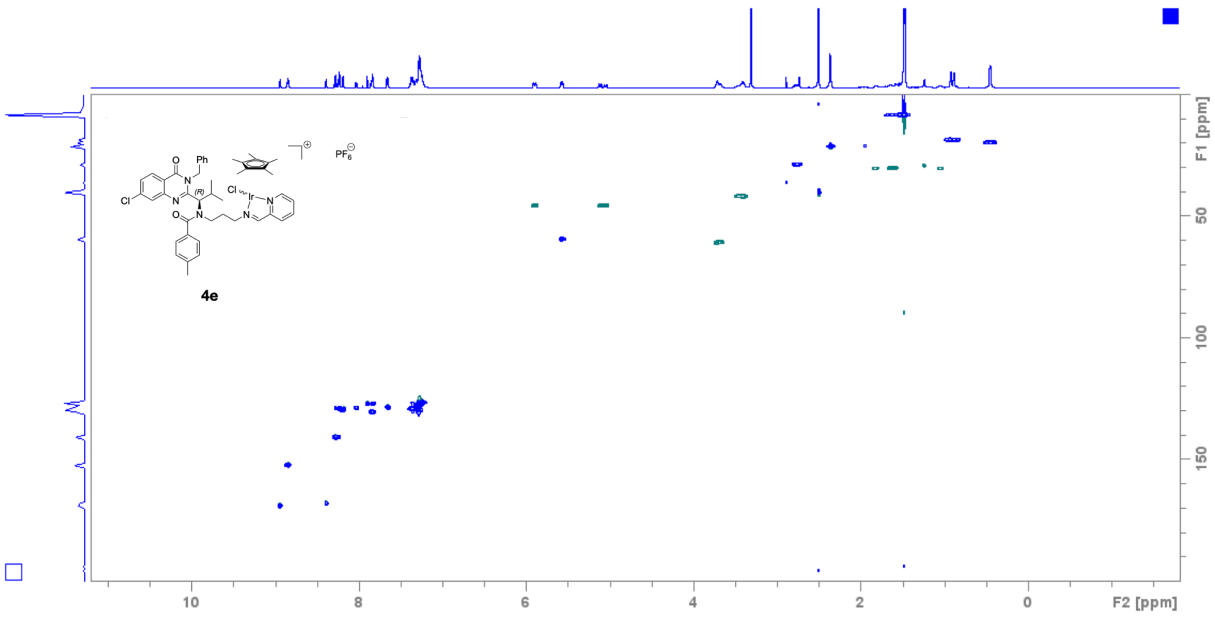

Supporting Figure S57. ^{1}H-^{13}C HSQC NMR of **4e** in DMSO-d_6

References

(1) Lowe, J.; Li, H.; Downing, K. H.; Nogales, E. "*Refined structure of alpha beta-tubulin at 3.5 A resolution*" *J. Mol. Biol.* **2001**, *313* (5), 1045-1057. DOI: 10.1006/jmbi.2001.5077.

(2) Berman, H. M.; Westbrook, J.; Feng, Z.; Gilliland, G.; Bhat, T.; Weissig, H.; Shindyalov, I. N.; Bourne, P. E. "*The protein data bank*" *Nucleic Acids Res.* **2000**, *28* (1), 235-242.

(3) Berman, H.; Henrick, K.; Nakamura, H. "*Announcing the worldwide protein data bank*" *Nat. Struct. Mol. Biol.* **2003**, *10* (12), 980-980.

(4) "*Scigress: Version FJ 2.6 (EU 3.1.7)* " *Scigress: Version FJ 2.6 (EU 3.1.7) Fujitsu Limited* **2008-2016**.

(5) Jones, G.; Willett, P.; Glen, R. C.; Leach, A. R.; Taylor, R. "*Development and validation of a genetic algorithm for flexible docking*" *J. Mol. biol.* **1997**, *267* (3), 727-748.

(6) Eldridge, M. D.; Murray, C. W.; Auton, T. R.; Paolini, G. V.; Mee, R. P. "*Empirical scoring functions: I. The development of a fast empirical scoring function to estimate the binding affinity of ligands in receptor complexes*" *J. Comput. Aided Mol. Des.* **1997**, *11* (5), 425-445.

(7) Verdonk, M. L.; Cole, J. C.; Hartshorn, M. J.; Murray, C. W.; Taylor, R. D. "*Improved protein-ligand docking using GOLD*" *Proteins* **2003**, *52* (4), 609-623. DOI: 10.1002/prot.10465.

(8) Korb, O.; Stutzle, T.; Exner, T. E. "*Empirical scoring functions for advanced protein-ligand docking with PLANTS*" *J. Chem. Inf. Model* **2009**, *49* (1), 84-96. DOI: 10.1021/ci800298z.

(9) Mooij, W. T.; Verdonk, M. L. "*General and targeted statistical potentials for protein-ligand interactions*" *Proteins* **2005**, *61* (2), 272-287. DOI: 10.1002/prot.20588.